Volume 2

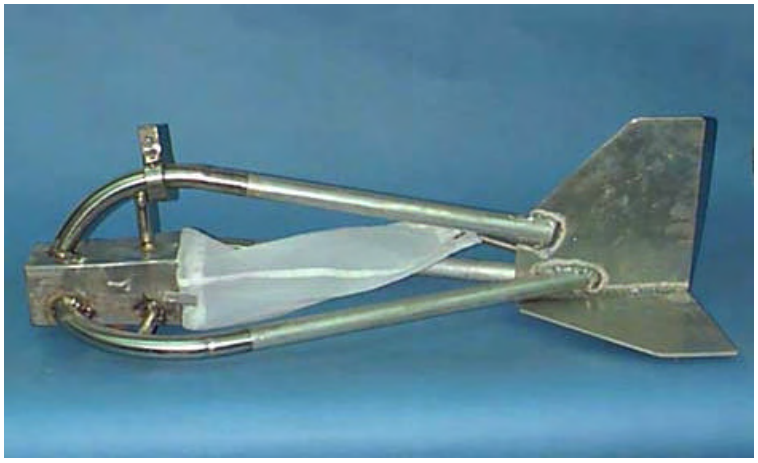

VI. Data Quality Assurance

VI. Data Quality Assurance

TABLE OF CONTENTS

ACCURACY, CONSISTENCY, and RELIABILITY of SEDIMENT MEASUREMENT and MANAGEMENT, and THEIR COSTS

Liu Chuang, Senior Program Analyst, Natural Resources Conservation Service, U.S. Department of Agriculture, Washington, D.C.

Liu Chuang, Room 6162, USDA South Building, phone: 202-720-7076, fax: 202-720-6473, liu-hsiung.chuang@usda.gov

INTRODUCTION

This paper aims to use one example of sediment measurement to convey the basic concepts of economic reasoning. Sediment measurement program is chosen for its general familiarity among participants in this conference.

Sediment is a phenomenon of soil erosion process, which generally starts with soil first being detached by wind or water, or other forces, then further transported and finally either becomes suspended particles in water or wind and finally settled on land surface. Sediment represents the soil quantity suspended or deposited.

Sediment has been cited to be the number one threat to American water quality. Sediment impairs fish respiration, plant productivity, and ecosystems of other marine life, and further limits the aesthetic, transportation, hydro-power and recreational usefulness of rivers and lakes.

Sediment information is used for measuring effects of changing agricultural practices, for engineering design of facilities, such as bridges, locks, dams, and hydropower structures, for reservoir study to help reservoir maintenance.

Measurement of sediment, like measurement of any other physical or non-physical matter and variables, always aims to provide accurate, consistent, and reliable estimates for users or potential users.

Accuracy on sediment measurement means measured sediment is close to actual amount of sediment one intends to measure, or the difference between sediment actually measured and the sediment intended to be measured becomes the minimum. In statistical terms, unbiased estimator of sediment measurement satisfies the requirement of accuracy.

Consistency on sediment measurement means methods and procedures used to measure sediment in different time and location should be the same, so comparison among the measured sediment value in different locations and times could be consistently compared. Consistency in statistical terms means that estimates of true sediment in a sample become closer to the true value of sediment when sample size becomes larger, or the variance of an estimated sediment value becomes smaller when the sample size increases.

Reliability has been used interchangeably with precision. It means that under same conditions of measurement, the method and procedures of sediment measurement would yield estimates of the expected value of the true sediment value repetitiously. In other words, it means an estimate from a more reliable estimator would have a higher probability of being close to the expected value than an estimate from a less reliable estimator. In general statistical terms, one would say that within a given interval, a more reliable estimator has less chance of producing an estimate outside of that interval than a less reliable estimator.

In principle the more accurate, consistent, and reliable sediment measurement, the larger a sample size and more effort will be needed. The more effort for sediment measurement means that more investment in resources for measurement and these include effort, human hours, instruments and materials. This will increase the costs of measurement.

THE FACTOR INPUTS AND PROCEDURES FOR SEDIMENT MEASUREMENT

Sediment data collection and management are just a small part of the earth-science data for which the USGS and other associated agencies and institutions are responsible. Sediment measurement involves several major tasks. These are 1) to monitor sediment transport in streams by collecting water samples at selected sites, 2) to measure suspended-sediment concentration in water, then 3) to estimate total suspended-sediment load flowing past a site, then 4) to publish information and data, and 5) to circulate and distribute these data and information to users.

In order to do the tasks described above, USGS and responsible agencies need to build monitoring stations and hire sediment observers in the country. Several steps are needed to build the monitoring stations. Planning and decision on site selection will first be made. Construction and installation of the monitoring site will then follow with the inspection and testing of the instruments. Simultaneously, sediment observers will be hired and trained by the USGS personnel.

The cost components of the sediment measurement primarily will consist of the following items:

A monitoring stream gagging shelter

Mechanical/electronic instruments in a shelter near stream will include:

Wire-weight gage (a drum with single layer of cable, bronze weight, a graduated disc, a counter, and a aluminum box)
Sediment sampler box,
Suspended sediment sampler,
Staff gage (monitor elevation/gage height of water on site)

Personnel of USGS do regular site visits at least every 6 weeks to (1) collect samples at the gage house or a specific site, and (2) restock supply of bottles, nozzles, gaskets, log sheets, markers, thermometers, or other supplies. They also conduct the analysis of the data being collected. To be more specific, to operate and maintain the site the USGS personnel have basic duties such as

1) To inform the sediment observer of the sampling strategy to follow at the site, like a fixed schedule (per day, per week, or month), or a schedule based on water discharge (like, sample 3 times per day during floods), and .

2) To provide supplies needed by the sediment observer to consistently collect accurate water sample and data.

3) To collect water samples (measure suspended sediment concentration (mg/l)) and to re-supply periodically for the monitoring station.

4) To estimate mean discharge, mean concentration, sediment discharge, and other variables as requested.

5) To publish the data, and circulate/distribute to audiences

In general, more samples will be collected during floods. These samples are critical to measure and compute, as well as to publish sediment records at these sites. Water sample collection by USGS sediment observer will involve a set of standard procedures. An observer would spend approximately 15 minutes per site per sampling. This results in about 5 hours per month actual time spent at each gage. This estimate does not include driving time. In general, an observer with one station receives $100 per month to collect 3 sample per week, and an additional sample for additional $7.50.

USGS pays the sample observer every 3 months or quarterly. Sediment observers should never risk injury to collect samples, and can call collect any time to USGS personnel on any concerns related to sampling. However, if there is an accident related to water sampling by the observer, USGS might have difficulty to escape responsibility for part or whole of the associated remedies.

THE PRODUCTION FUNCTION FOR SEDIMENT MEASUREMENT AND INFORMATION PRODUCTION

From the above discussion and explanation of the factor inputs and processes needed for producing sediment information, a simple production could then be hypothesized as follows:

Input in labor hour (L) includes:

- Staff time of USGS personnel in planning, contracting, inspecting, managing, and processing the payments to any contractors for site construction and installation, and procurement of supplies (L1).
- Staff time in hiring, training the sediment observer and in analyzing and processing sediment data for users (L2).
- Sediment observers' time to collect and record the water sample (L3).

Fixed and variable material capital inputs (K) include:

- Fixed capital investment in monitoring site evaluation, planning, and construction of the monitoring site (K1).
- Mechanical and electronic instruments (K2)
- Variable supplies for the site and monitoring activities (K3).

Management and technological factor input (A, B) will take into account the evaluation and selection of the site and all instruments, the design of all instruments used, and the knowledge and skills in the development and integration of all the personnel and material components.

Assuming S is the data and information of sediment report, then the above inputs for sediment monitoring could be structured into a simple production function as follows:

$$S= f (K, L)=AK+ BL$$

Where S= sediment data and information including mean discharge, sediment discharge, mean concentration, temperature, and others.

A and B are technology coefficient vectors for capital and labor, where A=A1, A2, and A3; B=B1, B2, and B3.

K, the capital inputs including both fixed (shelter site) and variable capital (instruments and supplies), where K=K1 +K2 +K3

L, the labor hours of all sediment management personnel and observers, sum of all labor hours, where L=L1+L2+L3.

The production function, as one can observe, is a technical or engineering relation between output and inputs. For any given set of inputs, the production processes are designed to yield the greatest output. Economists or engineers are interested in finding the maximum output for any given set of inputs in the production function.

Output, in our example here is the flow of sediment data and information generated by the combined efforts of all the personnel and material investment involved. The data and information of sediment could be expressed as an indexed output. Output could also be expressed as multi-products, such as water height, temperature, mean discharge, mean concentration, and sediment discharge. Material capital inputs could be considered as stock or flow concepts and they could be more than one kind as discussed previously. The same situation exists among different kinds of labor as expressed in labor hours that are flow concepts.

As technology changes, the parameters of the production function would also change. In a world of progress, both capital and labor quality would change along the time. Therefore, the hypothesized production function could be rewritten into the following:

$$S= F (K, L, A, B, t)$$

Where t is time, or time period,

S is the sediment output in time,
K is the capital input in time,
L is the labor input in time.

Data used to estimate parameters in the hypothyzed production function could come from time series or cross sectional data. Time series are from daily, monthly, quarterly and yearly data of both output and input series. Cross sectional data could come from, in our example, different sediment measurement stations across the country.

MINIMIZING THE ECONOMIC BURDEN OF SEDIMENT MEASUREMENT

Although no prices are given to the value of sediment measurement, and USGS is not selling the data for profit, we still could have a hypothetical or "shadow" price for the unit value of the sediment measurement to derive the expected total value of the sediment information for the country. The cost function of the sediment measurement will be derived from the production function we discussed. However, in a governmental setting, where the expected total cost of the sediment measures would be like any governmental project, it makes sense to minimize total cost for any given output of the sediment measures. By definition, the total cost will be the sum of all labor costs, capital costs and material cost together. Since we define 3 kinds of labor, there should have 3 levels of wages. Likewise, 3 kinds of capital will have 3 kinds of rental rate for them.

Minimize total cost $C=w1L1 +w2L2 +w3L3+K1r1+Kr2+K3r3$

Subject to production constraints where $S = f(K, L)=AK+ BL$ (1)
S is a given set of sediment measurement
$K=K1+K2+K3$
$L=L1+L2+L3$
$A=[A,A2,A3)$; $B=[B1,B2,B3]$
Ratios of factor costs = ratios of corresponding marginal productivity
$W1/W2=f'(L1)/f'(L2)$ (2)
$W1/W3= f'(L1)/f'(L3)$ (3)
$W1/r1=f'(L1)/f'(K1)$ (4)
$W1/r2=f'(L1)/f'(K2)$ (5)
$W1/r3=f'(L1)/f'(K3)$ (6)

There are 7 equations and are 7 unknowns. These equations could be transformed into a form that a production input such as labor and capital is a function of a set of factor price ratios plus the level of sediment measurement, such as L1=f1(w1/w2, w1/w3, w1/r1, w1/r2, w1/r3, S).

By multiplying individual cost rate (wage, or capital price) to the above equation, the above equation becomes: w1L1=w1f1(wage and capital rate ratios and S). The same procedure is applied to the other 5 equations to provide similar types of equations. Then, by summing all the 5 equations to derive the total cost function for sediment measurement as follows:

$$C=F(w1, w2, w3, r1,r2, r3, S)$$

The total cost therefore is a function of factor unit costs and total level of sediment measurement. The supply function of each factor for sediment measurement is equivalent to the marginal cost (MC) function of the total cost function, which can be expressed as L1=MC (individual factor unit costs, and the total unit cost of the sediment measurement.)

In order to minimize the total cost of the sediment measurement under a determined level of sediment measurement, the conditions should be observed:

> Ratios of factor costs = ratios of corresponding marginal productivity.
> Or, the value of marginal product of an input, like L1, should be equal to the value of marginal product of every other input used in the production of S.

For example: If the wage rate of USGS personnel is $40 per hour, while the wage rate of sediment observers is $20 per hour (as reported $100 for 5 hours in average), the unit cost ratio of these two types of labor input is 2. The ratio of having an incremental increase in sediment measurement by hiring additional USGS personnel and the incremental increase in sediment measurement by an additional sediment observer should be 2. In other words, the additional sediment measurement of a USGS personnel should be at least 2 times that of an sediment observer, otherwise it would not be economical.

In order to increase the accuracy, consistency and reliability of sediment measurement, more samples or more sediment measurement will need to be taken. This could come from hiring more sediment observers, increasing USGS supervisory and analytical personnel on the project, or building more sediment monitoring stations. For considering these options, the economic rule of thumb suggests that the unit cost ratios of each pair of factor inputs should be equal to the ratios of incremental sediment measurement information made with respect to the corresponding paired factor inputs.

ECONOMIC BURDEN AND REQUIREMENTS OF SEDIMENT MEASUREMENTS

Accuracy versus economic burden

Accuracy in sediment measurement means unbiased measurement in statistical terms. Let S' be the estimator of the hypothetically true sediment measurement S, two conditions should be met. The expected value of S' , or E(S'), should be equal to S. When the frequency of measurement reaching infinity, the expected value of sediment measurement will be equal to its hypothetical value. By definition in mathematical term, the accuracy or unbiased measurement could be written in the following equations:

$$E(S') = S \qquad (1)$$

$$E(S') = \int_{-\infty}^{\infty} S' f(S') \, dS' \qquad (2)$$

By definition of Equation 2 above, when frequency of measurement is large, then the measured average sediment will be equal or approximately approach to the true sediment measure the sediment design has been looking for.

To increase the frequency of sediment measurement we will have to require the sediment observer to get more water samples than originally agreed or planned. The implication of the requirement for accuracy is a higher variable cost of sediment measurement. Variable cost elements will include the hours spent by sediment observers, the USGS personnel time of monitoring and supervising the monitoring stations, the supplies such as water bottle, log paper, and markers. Frequent use of the fixed components of the monitoring stations will increase the depreciation of the instruments installed for the monitoring activities. The potential increase of failure rate of these instruments and equipment, the reliability of the monitoring station will be decreased.

Therefore, in the onset of the monitoring design it will be critical to decide the frequency and timing of water sample collection, especially in the planning stage. Good effort on this criterion will produce a better plan, better data for requesting needed budget, and certainly will yield more accurate estimate of the average sediment estimates for each station.

Consistency and reliability versus economic burden

Consistency means if the sediment average measures tend to become concentrated on the true value of the sediment average, or the hypothetically expected sediment average, the sediment monitoring station has been designed for. Consistency means that when sample size increases the estimated sediment average become closer to its true average, or become a more reliable estimate of the true value.

When an estimate is consistent, it becomes an efficient estimate with less variation, and it also becomes a more reliable estimate because the chance of accepting an false estimate as well as rejecting a true estimate becomes smaller. Therefore, consistency requires another statistical condition, that the variance of an estimate, S' , should becomes smaller and smaller when the sample size becomes bigger and bigger.

$$\text{Var}(S') \leq \text{Var}(S'')$$, where S' ' is alternative estimators of the sediment.

In brief, to gain more consistent and reliable estimates of the sediment averages, the sample size should be larger. Therefore, the cost, especially the variable cost of the monitoring activities of sediment will increase.

Reliability

Reliability is a statistic that shows the probability of having true value of sediment measured within a certain percentage range of the estimated sediment value, like 5%. This statistic is a component of accuracy and closely related to consistency of an estimated sediment value. Once the bias and distribution of a estimated sediment value have been determined, the predictive power, or reliability of the estimated sediment value of its true value can then be determined. To increase sample size will not only increase the accuracy and consistency of an estimate, but also the reliability of the predictive power of the measured sediment value. As we have discussed above, the increase of sample size certainly will increase the costs of sediment measurement. However, by choosing to measure more samples within a flooding period, fewer samples within a slow flow period from a stream, the sample design basically reduces the variance of the

estimated sediment value, and hence enhances its predictive power, or reliability, in estimating the true value of sediment.

CONCLUSIONS AND RECOMMENDATIONS

To increase accuracy, consistency and reliability of measuring suspended sediment in water, more sampling or larger samples in general will be needed.

Since sediment measurement is a public endeavor rather than a profit maximization activity, economic conditions for profit maximization will not be applied. Instead, cost minimization conditions by subjecting the total cost function to be under constraints of different levels of marginal productivity of sediment measurement should be considered.

The crucial economic conditions for weighing the choices of action to increase the frequency of water sampling and analysis activities are the ratios of unit cost of factor inputs for the sediment measurement. These factor inputs could be the estimated labor hours of USGS supervisory and analytical personnel and that of sediment observer, and the rental rate or cost of capital investment in water monitoring station and its associated electronic instruments as well as needed material supplies.

For better design in order to derive more consistent, unbiased, and reliable estimates of sediment measurement, it is crucial to incorporate the expected statistical parameters the audience or users of these measures consider acceptable. Also, the pre-knowledge and analysis of the production and cost function of entire set of measurement stations and their administrative and management support, and the trade-off in cost and productivity among all factor inputs in the sediment measurement system should be crucial in helping reducing costs of the sediment measurement.

REFERENCES

Bain, Lee J., Introduction to Probability and Mathematical Statistics, 1987, Duxbury Press, PP.58-59, PP.276-278, PP.283-284.

Johnson, Gary P. 1997, Instruction Manual for U.S. Geological Survey Sediment Observers, U.S. Geological Survey, Open-File Report 96-431.

Klein, Lawrence R., 1962, An Introduction to Econometrics, Prentice-Hall, Inc.PP.84-129

Liebhafsky, H. H., The Nature of Price Theory, 1963, the Dorsey Press. Inc., PP.119-194.

Mood, Alexander M., Graybill, Franklin A. Introduction to the Theory of Statistics, 1963, McGraw Hill Book Company, Inc. PP.172-175; PP.311-318; 248-334.

Scheaffer, Richard L, Mendenhall, William, and Ott, Lyman, 1990, Elementary Survey Sampling, Duxbury Press, PP.90-97.

A SPREADSHEET ANALYSIS OF SUSPENDED-SEDIMENT SAMPLING ERRORS

By John V. Skinner, Hydrologist
8129 Andreas Path, Seymour, IN 47274

Abstract: Accurate sampling of suspended sediment requires special conditions at the entrance of an upstream facing nozzle. Flow velocity within the nozzle must match the upstream velocity in the proximity of the opening. Unfortunately, meeting this exacting requirement is seldom possible. This paper presents a method for evaluating sampling errors at a single vertical in a flow cross-section. A popular spreadsheet format is used to analyze four hypothetical samplers with abnormal inflow characteristics. They are evaluated under three flow regimes and four sizes of sediment particles. The data verify the importance of using samplers with ideal characteristics. Among the hypothetical samplers, the one with excessively high intake rates is superior to those with abnormally low rates. Errors are greatest with the largest grains (0.45mm) moving in low flows.

INTRODUCTION

Assessing errors in sampling suspended sediment is difficult for users as well as designers of sampling equipment. Errors arise from many sources that include inadequate coverage of temporal and spatial variations in sediment discharge. The frequency of sampling must be adequate to document the most rapid changes in discharge. Spatial sampling must be adequate to account for point-to-point variations in sediment distribution within a river cross section. This report addresses another aspect of errors, namely their relation to intake characteristics of samplers. With growing diversity in sampling requirements, designers and users alike must sometimes embrace equipment with intake (filling rate) characteristics that are less than ideal. This report presents a method for estimating errors in depth integrating a single vertical. The method is applied to four hypothetical samplers with distinctly different intake characteristics.

In isokinetic sampling, flow approaches and then enters a sampler's nozzle without undergoing acceleration. Neither the speed nor direction of flow changes as water is captured and routed to the sampling container. In non-isokinetic sampling, errors arise from two sources stemming from discharge biasing and particle momentum. With discharge biasing, a point in a vertical contributes to a sample but the contribution is not proportional to the discharge at the point. In other words, the contribution is not velocity weighted. Regions of low flow may contribute disproportionately large fractions to a sample while regions of high flow contribute small fractions. The other error, particle momentum, stems from curvatures in streamlines as water accelerates to enter a nozzle. If inflow is hyperkinetic (nozzle flow exceeds approach velocity), streamlines converge on the nozzle but sediment particles, owing to their momentum, resist the converging forces and escape capture. Consequently, sediment concentration in the sample falls below that in the approaching flow. The action reverses in hypokinetic sampling when inflow is slower than approach velocity. In this case, sample concentration is erroneously high.

A sampling-error study conducted by the Federal Interagency Sedimentation Project (FISP, Report 3,1941) addressed discharge biasing but neglected particle-momentum errors. Later, data

on momentum effects were published (FISP, Report 5, 1941). The present report incorporates the momentum data in an error analysis, which is presented in a popular spreadsheet format.

The particle-momentum experiment was conducted in a recirculating flume filled with water and sediment particles sieved into narrow size ranges. The test section was fitted with two upstream-facing nozzles mounted side-by-side and symmetrically located in the test section. One nozzle was siphoned at isokinetic intake rates while the other was siphoned at rates ranging from hyperkinetic through isokinetic to hypokinetic. One at a time, four grain sizes of sediment were tested: 0.45, 0.15, 0.06 and 0.01 mm. Error data were presented as graphs, which have been converted to power-series equations for use in the spreadsheet. Figure 1 shows plots of the equations.

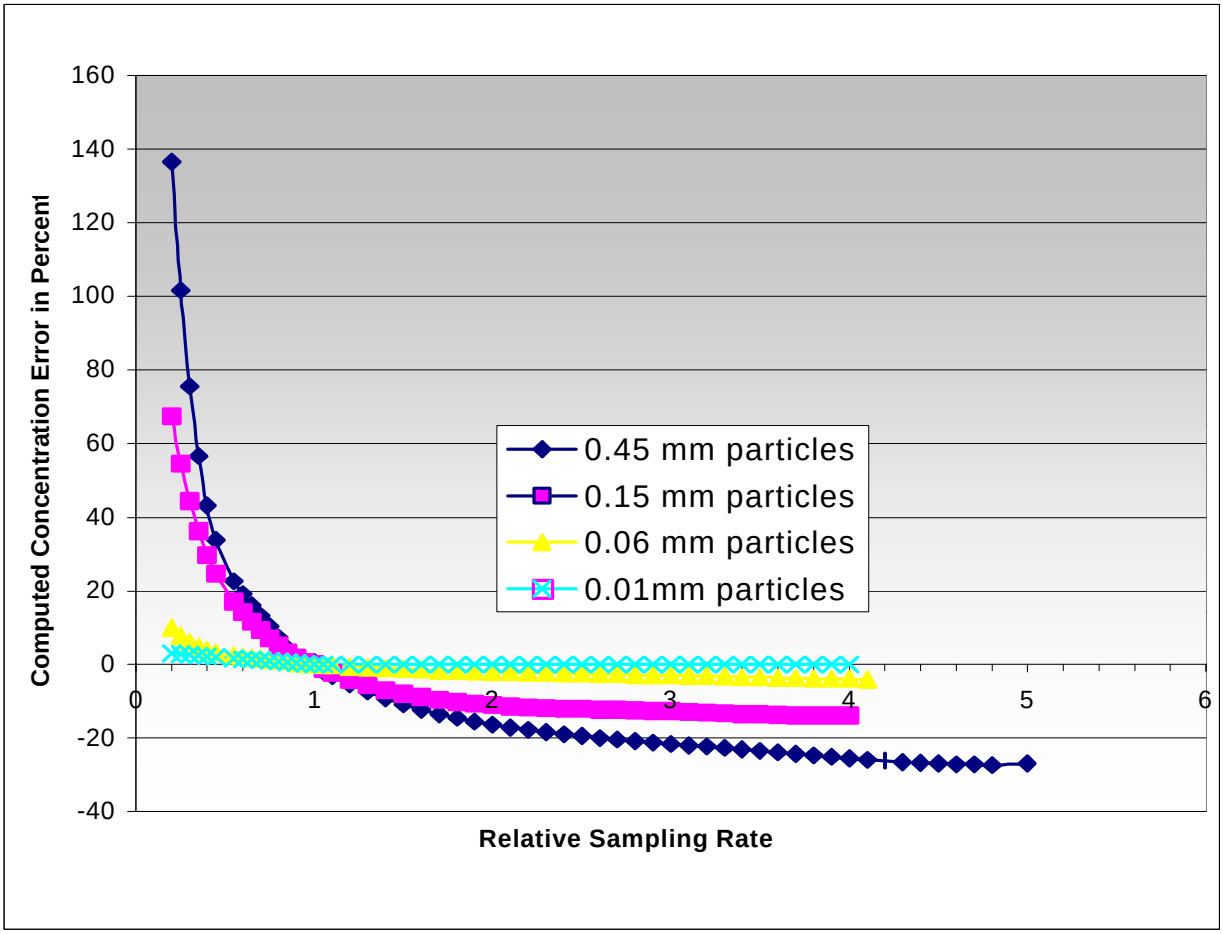

Figure 1--Particle-momentum sampling errors

In figure 1, *relative sampling rate* is the intake rate of the test nozzle divided by the isokinetic rate. Hyperkinetic rates plot to the right of 1.0; hypokinetic rates to the left. On the vertical axis, concentration errors are in percent with zero error occurring at a relative rate of 1.0. Errors are largest for the biggest grains, 0.45 mm. Errors are nearly insignificant at all relative sampling rates for the smallest grains, 0.01 mm. Within each grain size, errors are larger for hypokinetic rates than for hyperkinetic rates.

A sampler's intake characteristic is important in that it shows intake rates at various depths along a sampling vertical. Intake measurements are usually made in a laboratory flume. Water discharge is stabilized then flow velocity is measured at a test point chosen to minimize interference from the flume walls and surface waves. The current meter is then removed and the sampler is held at the test point for a measured time interval. After retrieving the sampler, the volume of water collected is measured. Intake rate is computed from the volume, the sampling interval and the cross-sectional area of the nozzle. Intake rate is plotted opposite the approach velocity, then flume discharge is set to a new level and the process is repeated. During development of a new sampler, intake characteristics are charted through a broad range of approach velocities, but once a sampler is in production, quality-control checks are usually made at only one or two points.

When a sampler operates at depths of several meters, as during actual river sampling, stringent controls must be observed to insure its intake characteristics apply. Descent speeds must allow for pressure equalization otherwise water floods the air-exhaust tube which, during proper operation, vents air from the sample container as water enters through the nozzle. Excessive rates of descent or ascent also create strong vertical currents, which interfere with smooth entrance flows. Limits on lowering and raising speeds, which are discussed in FISP publications, constrain a sampler's operating depth. Throughout this paper, it is assumed intake characteristics govern sampling operation at all depths.

Four hypothetical intake characteristics are shown in figure 2 and are analyzed in the spreadsheet. Scales on figure 2 are in ft/s to aid readers in comparing intake-characteristic plots in FISP publications. Units of ft/s can be converted to m/s by multiplying by 0.3048. On figure 2, an ideal sampler plots as "SI" with intake velocities matching approach velocities through a broad range. Points falling above the SI line are hyperkinetic: points below are hypokinetic. Sampler SL is hypokinetic through its full range. Furthermore, it stops sampling approach velocities slower than 1.5 ft/s (0.45 m/s). For approach velocities faster than 0.6 m/s, intake rates plot parallel to the ideal line, SI. Sampler SL has characteristics similar to some bag samplers in which stiffness of the bag prevents inflow in slow moving water. Sampler SR is also similar to some bag samplers that refuse to sample slow-moving water but are compensated through hyperkinetic operation at high velocities. This performance is achieved by creating strong suction pressures outside the bag. Sampler SF has an inflow velocity of 1.5 ft/s (0.45 m/s) in slack water. This operation is typical of many depth-integrating samplers, which have air-exhausts tubes opening above the intake nozzles. The intake of SF falls below the ideal for approach velocities higher than 3ft/s (0.9m/s). Sampler SH also samples in slack water but, unlike SF, it is hyperkinetic throughout its entire range. The four test samplers, SL, SF, SH and SR suffer from deficiencies that, for purposes of comparison, exaggerate shortcomings of production samplers. Characteristics of samplers in the U.S. series deviate from the ideal by only a few percent.

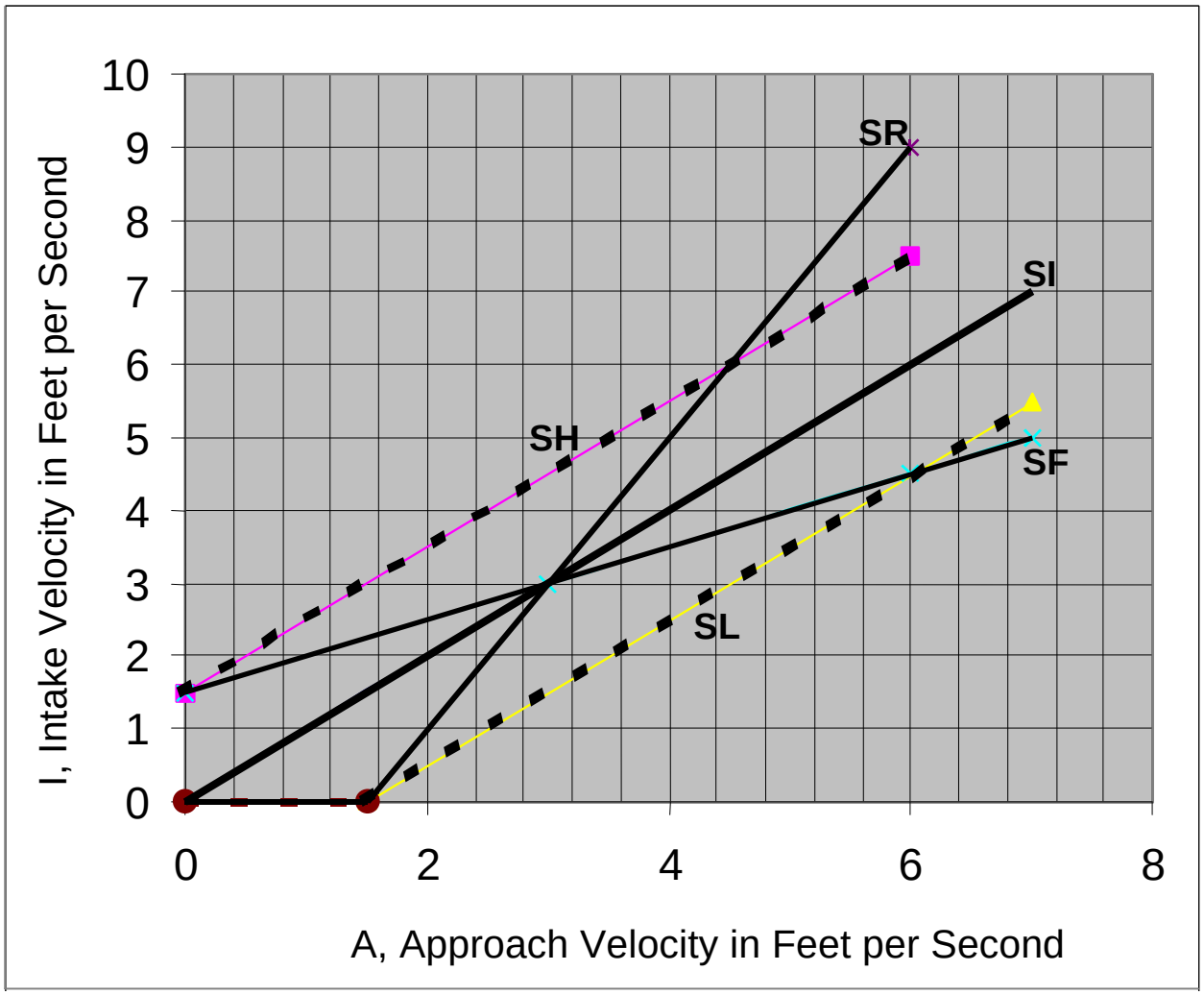

Figure 2--Intake characteristics of hypothetical test samplers

COMPUTATIONAL METHOD

The initial step in computing sampling errors is to assign constants listed in column A of the spreadsheet (figure 3). The first entry is the sampler type, SF in this case. The note is a reminder to enter the intake characteristic in equation form in all cells of column J. Returning to column A, the following parameters are listed in order (a) the sediment concentration at the stream bottom, (b) the fall velocity of the particle-size class, (c) Manning's roughness coefficient, (d) stream depth at the sampling vertical, (e) mean velocity in the vertical, (f) entrance diameter of the sampling nozzle and (g) the sampling interval in seconds for each segment of the vertical.

In the computations, the vertical is arbitrarily divided into twenty segments. As an approximation, velocities and concentrations are assumed equal at all points within a segment. Accuracy of the approximation can be improved at the expense of using more segments and working with larger spreadsheets. The segments are listed in column B with their boundaries shown as fractional depths with zero at the water surface and 1.0 at the stream bottom. Column C

Spreadsheet for SF Sampler, 0.45-mm Sediment and Low Flow

	A	B	C	D	E	F	G	H	I	J	K	L	M
1	ASSIGNED CONSTANTS	f, Fractional depth at sampling vertical (0 is surface, 1is bottom)	Relative height of segment boundaries above stream bed	Stream velocity at segment boundaries, ft/s.	A, Average velocity in segment. Also ideal sampler average intake velocity, ft/s	Q, For ideal sampler, volume of sample collected in interval, ml	Sediment concentration at segment boundary, mg/L	Average concentration in segment. Also for ideal sampler, concentration of sample in segment, mg/L	For ideal sampler, mass of sediment collected in segment, mg	Intake Velocity of test sampler (TS), ft/s	Volume of sample collected in interval by TS, ml	Relative sampling rate for TS	Sediment concentration error for TS, percent
2	Sampler type--SF. Insert intake characteristic equation in	0.00	1.00	2.63			0.00						
3	column J.	0.05	0.95	2.60	2.62	25.27	0.00	0.00	0.00	2.81	27.12	1.07	-2.41
4	No, Sediment Concentration at Stream Bottom, mg/L	0.10	0.90	2.57	2.58	24.94	0.00	0.00	0.00	2.79	26.96	1.08	-2.59
5	1000	0.15	0.85	2.53	2.55	24.60	0.00	0.00	0.00	2.77	26.79	1.09	-2.79
6	c, Fall Velocity of particles, cm/s.	0.20	0.80	2.49	2.51	24.25	0.00	0.00	0.00	2.76	26.61	1.10	-3.00
7	7.6	0.25	0.75	2.45	2.47	23.86	0.01	0.01	0.00	2.74	26.42	1.11	-3.23
8	n, Manning roughness coefficient	0.30	0.70	2.41	2.43	23.45	0.02	0.01	0.00	2.71	26.21	1.12	-3.48
9	0.04	0.35	0.65	2.36	2.38	23.02	0.04	0.03	0.00	2.69	25.99	1.13	-3.76
10	D, Stream depth at sampling vertical, ft.	0.40	0.60	2.31	2.33	22.55	0.08	0.06	0.00	2.67	25.76	1.14	-4.06
11	3	0.45	0.55	2.25	2.28	22.04	0.18	0.13	0.00	2.64	25.50	1.16	-4.40
12	Vm, mean velocity in vertical, ft/s	0.50	0.50	2.19	2.22	21.48	0.39	0.28	0.01	2.61	25.22	1.17	-4.78
13	2	0.55	0.45	2.13	2.16	20.87	0.86	0.62	0.01	2.58	24.92	1.19	-5.21
14	d, sampler nozzle diameter, in.	0.60	0.40	2.05	2.09	20.18	1.87	1.36	0.03	2.55	24.58	1.22	-5.71
15	0.25	0.65	0.35	1.97	2.01	19.42	4.11	2.99	0.06	2.51	24.19	1.25	-6.30
16	T, sampling time in each segment, s.	0.70	0.30	1.87	1.92	18.54	9.01	6.56	0.12	2.46	23.75	1.28	-7.01
17	1	0.75	0.25	1.76	1.81	17.51	19.75	14.38	0.25	2.41	23.24	1.33	-7.88
18		0.80	0.20	1.61	1.68	16.27	43.29	31.52	0.51	2.34	22.62	1.39	-9.00
19		0.85	0.15	1.43	1.52	14.71	94.91	69.10	1.02	2.26	21.84	1.48	-10.54
20		0.90	0.10	1.18	1.30	12.59	208.07	151.49	1.91	2.15	20.78	1.65	-12.83
21		0.95	0.05	0.74	0.96	9.23	456.15	332.11	3.07	1.98	19.10	2.07	-16.91
22		1.00	0.00	0.00	0.37	3.56	1000.00	728.08	2.59	1.68	16.26	4.57	-27.12
23													
24					Total volume collected by ideal sampler, ml	388.33		Total sediment mass collected by ideal sampler, mg	9.58	Total volume collected by test sampler, ml	483.85		
25													
26				Concentration of		24.66			Concentration of		39.73		
27				sample collected by					sample collected by				
28				ideal sample, rmg/L					test sampler, mg/L				

Figure 3–Sample spreadsheet for sampling errors in a vertical.

inverts the segment designation to simplify certain computations. The value 1.0 now designates the water surface and "0" the stream bottom.

Stream velocities at segment boundaries are computed in column D from the following velocity equation extracted from Report 3 (FISP, Report 3, 1941):

$$V = V_m [1+(9.5n/D^{1/6})(1+\log_e h)] \quad (1)$$

Where:

V is stream velocity at h,
V_m is mean velocity in the vertical,
n is Manning's roughness coefficient,
D is stream depth at the vertical, and
h is the ratio of the distance to a point above the streambed to the total depth at the vertical.

Equation 1 has the deficiency of yielding negative velocities *near* the streambed and an indeterminate value *at* the bed. Overriding the equation and inserting a value of zero at the bed circumvents this difficulty.

Column E shows mean velocities within the segments. Each mean is the average of two values: the velocity at the top of the segment and the velocity at the bottom. Mean values are displaced downward one cell so the entry for the top segment is in cell E3.

From velocities in each segment, the volume of water collected by the ideal sampler is computed. Inflow is isokinetic, so the volume (column F) is the product of stream velocity (column E), sampling time (1 second as entered in cell A17) and nozzle-entrance area.

Column G shows sediment concentration along the vertical as computed from the equation

$$N=N_o e^{-16th} \quad (2)$$

Where:

$$t = (0.0086cD^{1/6})/(nV_m) \quad (3)$$

In these equations, N is sediment concentration at relative elevation h,
N_o is sediment concentration at the streambed,
c is the fall velocity of the particle size class,
V_m is the mean velocity in the vertical,
n is Manning's roughness coefficient, and
D is stream depth at the vertical.

As with velocity data, concentrations are averages of values at the top and bottom of each segment. Concentrations within the segments are in column H. Computing sediment inflow to the ideal sampler is the next step. Because inflow is isokinetic, segment concentrations (column G) are multiplied by sample volumes (column F). The products are listed in column I.

Intake velocities for the test sampler SF are computed from its intake-characteristic equations and flow velocities within the segments (column E). Intake velocities, which are tabulated in column J, are then multiplied by nozzle area and sampling time to obtain sample volumes in column K. Relative sampling rates, calculated as intake velocities (column J) divided by stream velocities (column E), are tabulated in column L. From relative-sampling rates and particle size (0.45 mm), concentration errors (figure 1) are computed in column M.
Concentrations entering the test sampler are computed from concentrations within the segments (column H) and concentration errors from column M. Results rounded to two decimal places are listed in column N. Sediment masses collected by the test sampler are computed from concentration data in column N and sample-volume data in column K. Masses rounded to two places are listed in column O.

Properties of the composite samples representing the entire vertical are computed from data for individual segments. The composite volume collected by the ideal sampler is the sum of data in column F. The total is in cell F24. The composite volume collected by the test sampler is the sum of data in column K. The total is in cell K24. Total sediment mass collected by the ideal sampler is the sum of data in column I. The total is in cell I24. Total sediment mass collected by the test sampler is the sum of data in column O. The total is in cell O24. Concentrations of the composites are computed as the ratio of total sediment mass to total sample volume. Results for the ideal and test sampler are in cells F26 and O26 respectively.

All computations are based on equations which do not appear on spreadsheet printouts but are embedded in the cells. These equations may be obtained at the Internet site http://fisp.wes.army.mil.

SUMMARY OF RESULTS

Sampling errors for complete verticals are listed in the upper half of table 1. High flow is arbitrarily taken as a depth of 10 ft (3.05 m) and a mean velocity of 6 ft/s (1.83 m/s); medium flow is 6 ft (1.83 m) and 4 ft/s (1.22 m/s); low flow is 3 ft (0.91 m) and 2 ft/s (0.61 m/s). The bottom half of table 1 shows errors with an unsampled zone approximated by deleting data for the bottom segment for the ideal and test samplers.

Table 1 shows sampler SH is superior in every category of particle size, flow regime and integration depth. The sampler's hyperkinetic intake rate guarantees that all segments are sampled to some degree even though intake rates are not discharge weighted. However, sampler SH has significant errors, which are greatest in a combination of low flow and maximum grain size. The data verify the importance of using samplers with isokinetic or nearly isokinetic characteristics. In terms of concentration, over-sampling (positive errors) can occur within every segment, yet under-sampling (negative errors) can occur for the composite sample representing the entire vertical. The combination of positive and negative errors stems from volumetrically over-sampling segments near the surface where, compared to segments near the bed, particles are present in low concentrations. The excessive inflow from the surface dilutes the entire sample to produce an erroneously low concentration.

Across particle sizes, errors increase with shifts toward larger grains. Because of their high fall velocities, large particles concentrate near the bottom. Errors in sampling lower segments mask inflows from the remaining portion of the vertical. Eliminating the bottom segment (lower half of table 1) reduces errors but at the expense of ignoring transport near the bed.

Table 1--Rank of samplers by concentration errors. Samplers are listed in order of absolute error with the most desirable (smallest error) at the head of each category. Percent errors with signs are in parenthesis.

Percent of depth sampled	**Grain Size**											
	0.45 mm			0.15 mm			0.06 mm			0.01 mm		
	High Flow	Med. Flow	Low Flow	High Flow	Med. Flow	Low Flow	High Flow	Med. Flow	Low Flow	High Flow	Med. Flow	Low Flow
100	SH (1.3)	SH (7.0)	SH (35.0)	SH (-2.9)	SH (-2.3)	SH (7.2)	SH (-0.1)	SH (0.3)	SH (2.7)	SH (0.0)	SH (0.1)	SH (0.2)
	SL (-7.2)	SL (-14.8)	SF (61.0)	SL (3.0)	SL (3.6)	SF (16.7)	SL (0.1)	SL (-0.7)	SF (5.4)	SR (-0.1)	SR (-0.1)	SF (0.3)
	SF (22.6)	SF (28.8)	SL (-83.0)*	SF (10.4)	SF (9.4)	SL (-20.0)*	SF (2.3)	SF (2.7)	SL (-9.2)	SL (0.8)	SF (0.6)	SR (0.4)
	SR (-25.5)	SR (-35.2)	SR (-88.4)*	SR (-11.6)	SR (-13.0)	SR (-36.3)	SR (-2.4)	SR (-3.3)	SR (-12.4)	SF (1.0)	SL (1.2)	SL (1.7)
95	SH (-2.0)	SH (-0.4)	SH (8.1)	SH (-3.4)	SH (-3.7)	SH (-0.2)	SH (-0.3)	SH (-0.1)	SH (1.4)	SH (0.0)	SH (0.1)	SH (0.1)
	SL (2.3)	SL (-1.5)	SF (24.7)	SL (4.6)	SL (5.9)	SF (8.4)	SL (0.4)	SL (-0.2)	SF (3.6)	SR (0.0)	SR (-0.1)	SF (0.2)
	SF (17.3)	SF (17.4)	SL (-76.9)*	SF (9.6)	SF (7.4)	SL (-16.6)	SF (2.0)	SF (2.1)	SL (-8.5)	SL (0.8)	SF (0.6)	SR (0.4)
	SR (-17.9)	SR (-25.1)	SR (-84.2)*	SR (-10.3)	SR (-11.1)	SR (-33.5)	SR (-2.1)	SR (-2.8)	SR (-11.7)	SF (1.0)	SL (1.2)	SL (1.8)

*Errors are estimated because some relative sampling rates fall beyond experimental limits.

REFERENCES

Federal Interagency Sedimentation Project, 1941, Analytical study of methods of sampling suspended sediment--Interagency Report 3, Iowa City, Iowa University Hydraulics Laboratory, 82 p.

Federal Interagency Sedimentation Project, 1941, Laboratory investigation of suspended sediment samplers--Interagency Report 5, Iowa City, Iowa University Hydraulics Laboratory, 99p.

COMPUTATION OF SUSPENDED-SEDIMENT CONCENTRATIONS IN STREAMS

David J. Holtschlag, Hydrologist, U.S. Geological Survey, Lansing, Michigan
6520 Mercantile Way, Suite 5, Lansing, Michigan 48911
voice: (517) 887-8910; fax: (517) 887-8937; email: djholtsc@usgs.gov

Abstract Optimal estimators are developed for computation of suspended-sediment concentrations in streams. The estimators are a function of parameters, computed by use of generalized least-squares regression, that simultaneously account for effects of streamflow, seasonal variations in average sediment concentrations, a dynamic error component, and the uncertainty in concentration measurements. The parameters are used in a Kalman filter for on-line estimation and an associated smoother for off-line estimation of suspended-sediment concentrations. The accuracies of the optimal estimators are compared with alternative interpolation and regression estimators by use of long-term daily-mean suspended-sediment concentration and streamflow data from 10 sites within the United States. For sampling intervals from 3 to 48 days, the standard errors of on-line and off-line optimal estimators ranged from 52.7 to 107 percent, and from 39.5 to 93.0 percent, respectively. The corresponding standard errors of linear and cubic-spline interpolators ranged from 48.8 to 158 percent, and from 50.6 to 176 percent, respectively. The standard errors of simple and multiple regression estimators, which did not vary with the sampling interval, were 124 percent and 105 percent, respectively. Thus, the off-line estimator (smoother) had the lowest error characteristics among the estimators evaluated. Because suspended-sediment concentrations are typically measured at less than three-day intervals, use of optimal estimators will likely result in significant improvements in the accuracy of continuous suspended-sediment concentration records. Additional research on the integration of direct suspended-sediment concentration measurements and optimal estimators applied at hourly or shorter intervals is needed.

INTRODUCTION

Computation of average sediment concentrations and flux rates requires the integration of continuous data on streamflow with discrete measurements of sediment concentration. This integration is commonly carried out by interpolating discrete measurements by use of time-averaging or flow-weighting methods. Phillips *et al.* (1999) compared 20 existing and two proposed methods for computing loads and found that a time-averaging method produced the most precise estimates for two stations analyzed. The precision of this method decreases significantly, however, as the sampling interval increases (Phillips*et al.*, 1999). Furthermore, Bukaveckas *et al* (1998) conclude that time-averaging methods may produce biased estimates of flux during periods of variable discharge.

A sediment-rating curve approach (Helsel and Hirsch, 1992) is a common method of flow weighting. A rating curve generally describes the relation between the natural logarithms (logs) of suspended-sediment concentration and the logs of streamflow. This rating-curve approach, however, has been found to underestimate river loads (Ferguson, 1986). In addition, Bukaveckas *et al* (1998) indicate that flow-weighting methods may produce biased estimates if the concentration-streamflow relation is affected by antecedent conditions or has seasonal variability. Seasonal rating curves are used to reduce the scatter and to eliminate this bias at some sites (Yang, 1996).

Purpose and Scope This paper develops optimal on-line and off-line estimators of suspended-sediment concentrations for streams on the basis of daily values of computed suspended-sediment concentration and flow information. Data from 10 sites are used to compare the accuracy of the optimal estimators with interpolation and regression estimators (Koltun, Gray, and McElhone, 1994) that are commonly used to compute suspended-sediment concentration records. The estimators were restricted to those that could be readily implemented with data that are generally available at gaging stations. The choice of daily-value, rather than unit-value (hourly or less) computational intervals, however, was based on the greater accessibility of daily-values data. The estimators are intended, however, for eventual application at unit-value intervals.

Site Selection: Ten USGS gaging stations (table 1) were selected to develop the estimators and assess their accuracy. The sites represent a broad range of basin sizes, suspended-sediment-concentration characteristics, and streamflow characteristics. Basin drainage areas range from 1,610 to 116,000 square kilometers (km^2). Median suspended-sediment concentrations range form 8 to 3,040 milligrams per liter (mg/L). Median streamflow ranged from 0.34 to 241 cubic meters per second (m^3/s). Available suspended-sediment particle-size distribution data indicates that the percentage of suspended sediment finer than 0.125 millimeters (mm) ranged from 70 percent to 95 percent among sites.

Table 1. Identification and location of selected sediment gaging stations

USGS station number	Station name	Basin area (square kilo-meters)	Latitude	Longitude	Record used in analysis Mo/Da/Year Begin date (End date)	Process variance, based on a measurement variance of 0.04.
01567000	Juniata River at Newport, PA	8,687	40°28'42"	77°07'46"	7/29/1952 (9/30/1989)	0.1357
01638500	Potomac River at Point of Rocks, MD	25,000	39°16'25"	77°32'35"	7/12/1966 (9/30/1989)	0.1015
01664000	Rappahannock River at Remington, VA	1,610	38°31'50"	77°48'50"	7/9/1965 (9/30/1993)	0.2893
02116500	Yadkin River at Yadkin College, NC	5,910	35°51'24"	80°23'10"	1/3/1951 (9/30/89)	0.1421
02131000	Pee Dee River at Peedee, SC	22,900	34°12'15"	79°32'55"	9/25/1968 (9/30/1972)	0.0799
02175000	Edisto River near Givhans, SC	7,070	33°01'40"	80°23'30"	3/26/1967 (9/30/1972)	0.1959
09180500	Colorado River near Cisco, UT	164,00	38°48'38"	109°17'34"	51/1968 (9/30/1984)	0.1665
09315000	Green River at Green River, UT	116,000	38°59'10"	110°09'02"	9/19/1968 (9/30/1984)	0.1025
09379500	San Juan River near Bluff, UT	59,600	37°08'49"	109°51'51"	12/17/1951 (12/3/1958)	0.1127
09382000	Paria River at Lees Ferry, AZ	3,650	36°52'20"	111°35'38"	10/1/1948 (9/30/1967)	0.5496

ESTIMATORS OF SUSPENDED-SEDIMENT CONCENTRATIONS

Previous estimators used to compute continuous records of suspended-sediment concentrations (Koltun, Gray, and McElhone, 1994) include both interpolators and linear regression models. Interpolators provide a simple method of filling in missing observations between suspended-sediment concentration measurements, which are typically obtained at unequal time intervals. These estimators have no rigorous mechanism for quantifying the uncertainty of the computed values, but provide estimates that are consistent with data at times of direct measurements. Linear regression models condition estimates of suspended-sediment concentrations on streamflow (and sometimes other explanatory variables), but do not converge properly to observed values at times of direct measurements. This paper describes estimators that integrate the benefits of both interpolators and linear regression estimators.

A natural logarithmic (log) transformation is commonly applied to suspended-sediment concentration and streamflow data to create more symmetrically distributed random variables prior to statistical analysis. Model development then proceeds in the transformed metric, which more closely satisfies underlying statistical assumptions. Estimation of suspended-sediment concentrations, which requires an inverse transformation of log concentrations back to the units of measurement, may introduce a bias in the

estimation procedure. Walling and Webb (1988) show that exponentiated estimates that are adjusted for this possible bias are significantly less accurate and less precise than estimates that are not adjusted, based on load calculations derived from rating curves.

Interpolators: Both linear and nonlinear interpolation is used to compute daily suspended-sediment concentrations from unequally-spaced measurements (Koltun, Gray, and McElhone, 1994). Interpolation provides estimates that match direct measurements of concentration exactly. Linear interpolations are linear in time between log-transformed concentrations. Nonlinear interpolation is based on a cubic spline function between log-transformed values. This interpolation produces a continuously differentiable arc that approximates a manually drawn curve. Estimates of concentrations from interpolations are obtained by inverse log transformation (exponentiation).

Regression Estimators: Regression estimators provide a statistical model for computing the magnitude and uncertainty of suspended-sediment concentrations. These models describe a static statistical relation between suspended-sediment concentrations and a corresponding set of explanatory variables. Explanatory variables are selected based on their correlation with suspended-sediment concentrations and their general availability. Once developed, regression equations are used to estimate suspended-sediment concentrations during periods when direct measurements are unavailable.

Simple linear regression *[slr]* equations developed in this paper for computing logs of suspended-sediment concentrations included an intercept term and a term containing the logs of streamflow. Results indicate that the logs of suspended-sediment concentrations were consistently positively related to the logs of streamflow, although the proportion of variability accounted for by streamflow varied widely among sites. The *slr* estimator described a minimum of 1.1 percent of the variability in logs of suspended-sediment concentrations at Edisto River near Givhans, S.C., and a maximum of 51.4 percent of the variability in logs of suspended-sediment concentrations at Paria River at Lees Ferry, Ariz. Residuals of all *slr* equations were highly autocorrelated, thus violating the assumption of independent residuals associated with ordinary least-squares regression.

Multiple linear regression [*mlr*] equations for computing suspended-sediment concentrations included an intercept term, a term containing the logs of streamflow, a term containing the changes in streamflow rate, and a first-order Fourier approximation of the annual seasonal component. In the *mlr* equations, the coefficients associated with the logs of streamflow were positive, indicating a direct relation between streamflow and suspended-sediment concentrations. In addition, with the exception of Paria River at Lees Ferry, Az., positive changes in daily streamflow were associated with increasing suspended-sediment concentrations. Finally, a seasonal component in logs of suspended-sediment concentrations was consistently detected at all sites. Conditioned on streamflow, the day of lowest average suspended-sediment concentrations was February 15 and the corresponding day of highest average concentrations was August 17. The amplitude of the seasonal component varied from a maximum of 1.0463 (in log of mg/L units) at Potomac River at Point of Rocks, Md., to a minimum of 0.2467 at Pee Dee River at Peedee, S.C. Similar to the *slr* results, significant autocorrelation was present in the residuals of *mlr* estimates.

State-Space Estimators: State-space models provide a basis for optimal estimation, that is the minimizing of error in the estimate of the state by utilizing knowledge of system and measurement dynamics, of system and measurement error variances, and initial condition information (Gelb, 1974, p. 2). State-space models disaggregate a dynamic system such as suspended-sediment concentrations into process and measurement components. The process component describes the evolution of the system dynamics and their associated uncertainty. The measurement component describes the static effects of explanatory variables and the uncertainty in the measurement process. Together, these components form an estimator that continually accounts for the effects of known inputs (such as streamflow) and optimally adjusts model estimates for periodic direct measurements that contain some uncertainty.

The process of adjusting for direct measurements is described as predicting, filtering, or smoothing, depending on the set of direct measurements used in estimation. Predicting uses only measurements prior to the time of estimation; filtering uses only measurements up to and including the time of estimation; and smoothing uses measurements before and after the time of estimation. Predicted and filtered estimates provide on-line data, that is, information that can be continuously updated to the present (real time). Smoothed estimates provide off-line data only, that is, estimates are delayed until subsequent direct measurements become available. The accuracy of off-line estimates, however, is generally greater than that of corresponding on-line values. Both on-line and off-lines estimators will be developed and analyzed in this paper, although the off-line estimators are of primary interest for publication of suspended-sediment concentrations.

Parameters of the state-space models were estimated by use of generalized least-squares regression. The generalized least-squares [*gls*] model contains two equations. The first equation describes the static dependency of suspended-sediment concentrations on the explanatory variables, and is similar in form to the multiple regression equations described previously. The second equation describes the dynamic error characteristics as a p^{th}-order autoregressive process. The parameters relating suspended-sediment concentrations to the explanatory variables and describing the autoregressive error characteristics were estimated iteratively by specification of the maximum likelihood option in the SAS/ETS® AUTOREG[1] procedure (SAS Institute, 1988, p.177).

Results of generalized least-squares regressions indicate that the statistical significance of the explanatory variables (streamflow, change in streamflow, and an annual seasonal component) is maintained with the inclusion of an equation describing the dynamic error component. Further, a $p=1$ (first order) autoregressive process was sufficient to describe the dynamic error characteristics at all selected sites. The root mean square error (RMSE) of residuals, from predicting logs of suspended-sediment concentration one day in advance of the current time step were significantly lower than the residuals from the corresponding multiple-regression equations. The coefficient of determination of the full model, including both static and dynamic components, improved significantly, while the autocorrelation of the residuals were diminished greatly.

Once the parameters of the state-space model were estimated, the error component was disaggregated into process error and measurement error subcomponents. Both subcomponents were assumed to be normally distributed independent sequences with expected values of zero and unknown variances. Estimates of individual measurement error variances can be computed by use of direct suspended-sediment concentration measurements following methods described by Burkham (1985). In this paper, however, daily values rather than direct measurements of suspended-sediment concentrations were used for model development, so it was necessary to use an average measurement variance, specified here as 0.04 mg^2/L^2 (about 20 percent). This approximation is not thought to have significantly impacted the results, as the final estimates have low sensitivity to the estimate of the measurement variance. Initial estimates of the process variances were computed as the difference between the residual variances of the generalized least squares equations and the assigned measurement variance. Final estimates of the process variance were adjusted so that the lead 1 forecast intervals contained 95 percent of the measurements for an alpha (type 1 error) value of 0.05 (Siouris, 1996, p. 139).

On-Line Estimation: The Kalman filtering algorithm (Grewal and Andrews, 1993) computes on-line estimates of suspended-sediment concentrations by use of a state-space model. The algorithm involves a two-part computation: a temporal projection, determined by the system dynamics and the process variance, and a measurement update, determined by the magnitude of the measured suspended-sediment concentrations and the measurement variance. The filter is initiated by use of an estimate of the state and

[1] Use of trade names in this paper is for identification only and does not constitute endorsement by the U.S. Geological Survey.

its variance at time zero. In the process of filtering, a Kalman gain is computed that optimally weights the reliability of the model with the reliability of the measurement data and causes the initial estimates of the state and its variance to converge to optimal values. Ordinarily, computations for the temporal projection and measurement update alternate, causing the state error variance to alternatively increase and decrease. If no measurement data is available for a particular interval, however, the measurement update is skipped and the state and its variances are maintained from the previous temporal projection.

Off-Line Estimation: A smoother is a mathematical procedure that combines a forward running filter estimate with a backward running filter estimate. Thus, all data before and after the time for which the estimate is computed, is used to determine an optimal value. Smoothers are based on more data than forward running filters and are generally more accurate. Smoothing is considered an off-line estimation procedure because estimates are delayed until measurements at the end of the estimation intervals become available. In this application, a fixed-interval smoother, which provides optimal values of all states within an estimation interval defined by beginning and ending measurements, is computed by an algorithm referred to as the Rauch-Tung-Striebel (RTS) smoother (Gelb, 1974, p. 164, Grewal and Andrews, 1993, p. 155). To implement the smoother, the Kalman filter is run up to the measurement ending the estimation interval. All state and variance elements computed by the forward-running (Kalman) filter are subsequently utilized by the backward-running filter. In particular, the initial condition for the smoother is the filter estimate formed by the measurement update at the end of the estimation interval. A smoother gain is computed and the smoother runs backward in time updating filter estimates of the state and state error variance.

Comparison of Estimators

Techniques for estimation of suspended-sediment concentrations described in this paper include interpolation, regression, and optimal estimators. Figure 1 provides a graphical comparison of some of these estimators for the hypothetical situation in which only 1 of 12 daily values is available to estimate the complete record. Results for the interpolation techniques, which are represented here by cubic-spline interpolation, indicate that interpolation fits the selected (direct) measurements, but fails to account for streamflow influences and often results in a poor match between the estimates and suspended-sediment concentrations not used in the estimation. Similarly, simple linear regression may result in poor estimates because it fails to adequately account for the concentration measurements used in estimation, even though the estimates are all conditioned on streamflow. Optimal estimators, represented by the off-line [Smoother] estimator, effectively accounts for streamflow (and seasonal) influences, and for information provided by (direct) measurements used in the estimation. In addition, the optimal estimators provide a measure of uncertainty of the estimated record (fig. 2).

In addition to a graphical comparison, summary statistics were computed to facilitate comparison of the accuracies of the alternative estimators. Specifically, the accuracies of simulated sampling intervals of 3, 6, 12, 24, and 48-days, separated by corresponding estimation intervals of 2, 5, 11, 23, and 47 consecutive unsampled days were investigated. The interpolators, filters, and smoothers were updated using data from the sampled days, and the accuracy of the estimators was assessed on the basis of RMSE of log concentration estimates on unsampled days. Results indicate that the off-line [*Smoother*] estimator was the most accurate (Fig. 3). Although the accuracy of the interpolators was high at shorter sampling intervals, this accuracy decreased rapidly with increasing sampling interval. The accuracy of regression estimators did not improve locally in response to direct measurements of suspended-sediment concentrations.

The RMSE can be expressed either in log units (as above) or as a standard error in percent. The RMSE in percent reflects the coefficient of variation of the estimator as:

$$RMSE_{Percent} = 100 \times \frac{s_y}{m_y} = 100 \times \sqrt{e^{s_y^2} - 1}$$

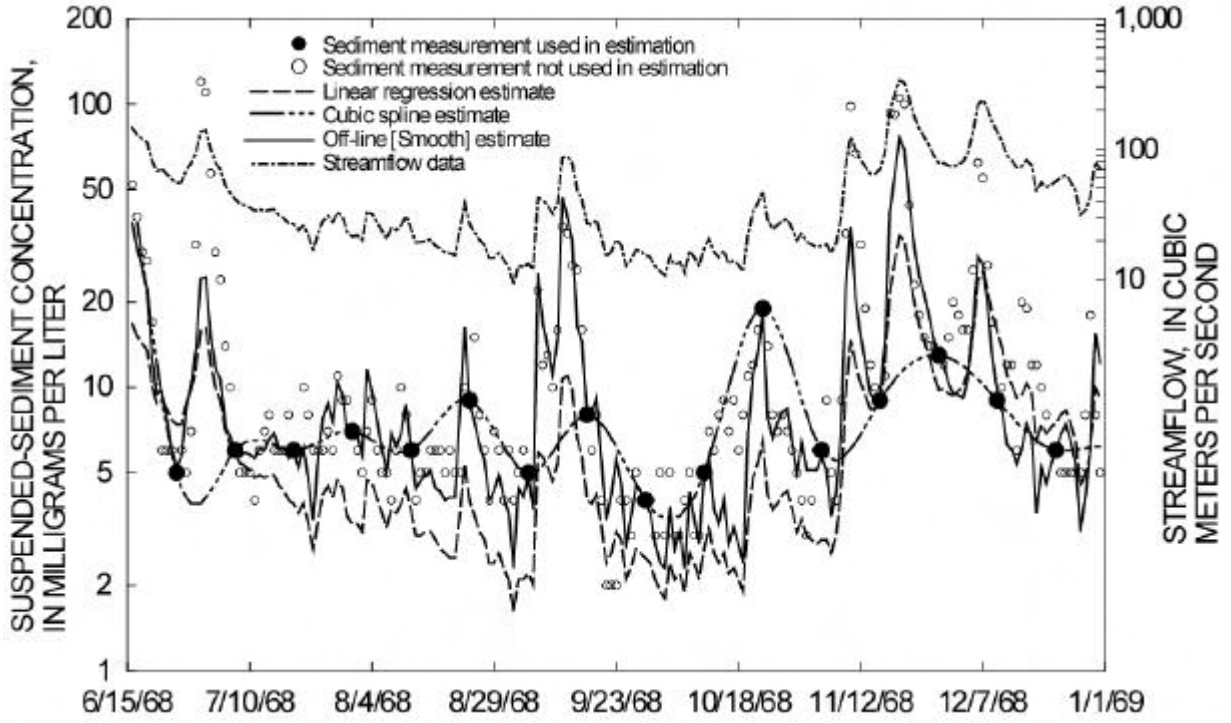

Figure 1. Suspended-sediment concentration and streamflow at Juniata River at Newport, Penn. (U.S. Geological Survey gaging station 01567000)

Results from this analysis indicate that the average standard error for the *slr* estimator is 124 percent and that the average standard error for the *mlr* estimator is 105 percent. The average standard error of the linear interpolator ranged from 48.4 percent for 3-day sampling intervals to 159 percent for 48-day sampling intervals. The average standard error of the cubic spline interpolator ranged from 50.6 percent for 3-day sampling intervals to 176 percent for 48-day sampling intervals. The average standard error for the on-line [*Filter*] estimator ranged from 52.7 percent for a 3-day sampling interval to 107 percent for 48-day sampling interval. The average standard error for the off-line [*Smoother*] estimator ranged from 39.9 percent for a 3-day sampling interval to 93.0 percent for a 48-day sampling interval. Thus, the off-line [*Smoother*] estimator has the lowest standard error, especially at the shorter sampling intervals that are needed to compute continuous records of suspended-sediment concentrations.

Possible sources of systematic variation in estimation errors among sites were investigated. In particular, off-line root-mean-square errors showed a slight tendency to decrease with increasing median discharges. Although the number of sites analyzed is thought to be too small to provide conclusive results, the finding is consistent with results by Phillips *et. al.* (1999), who indicated that the accuracy and precision of the estimators that they evaluated declined with a reduction in drainage area. No relation between model errors and sediment characteristics was detected.

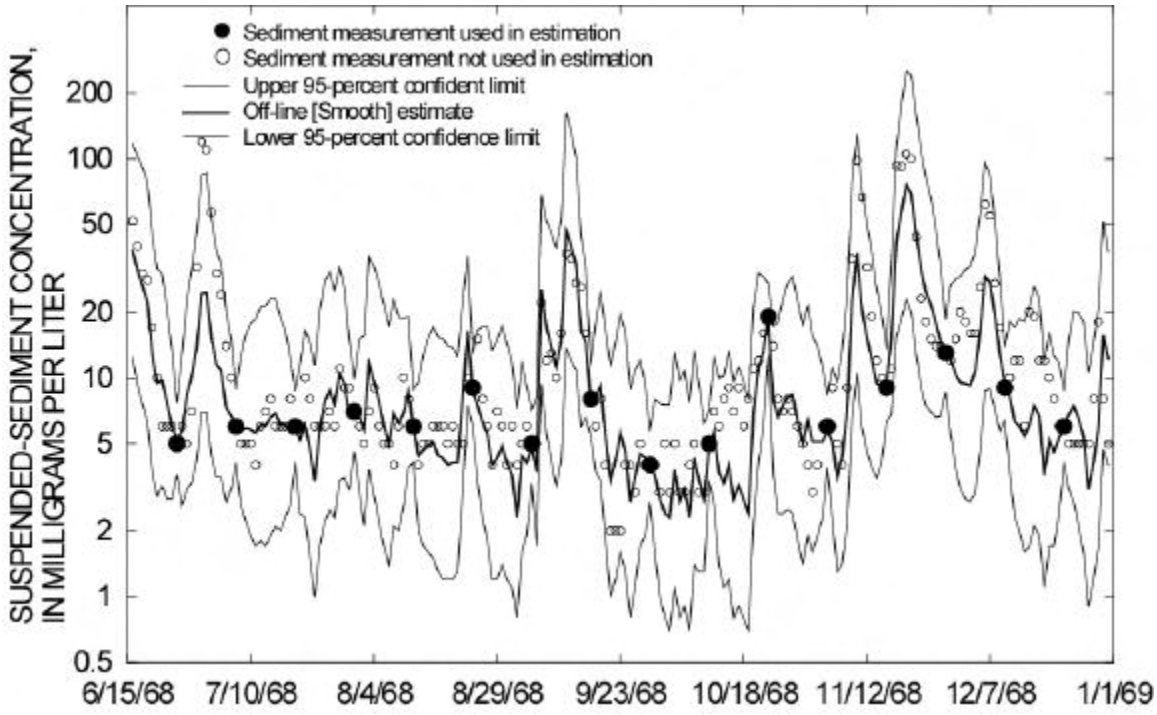

Figure 2. Estimates and uncertainties of suspended-sediment concentrations at Juniata River at Newport, Penn. (U.S. Geological Survey gaging station 01567000)

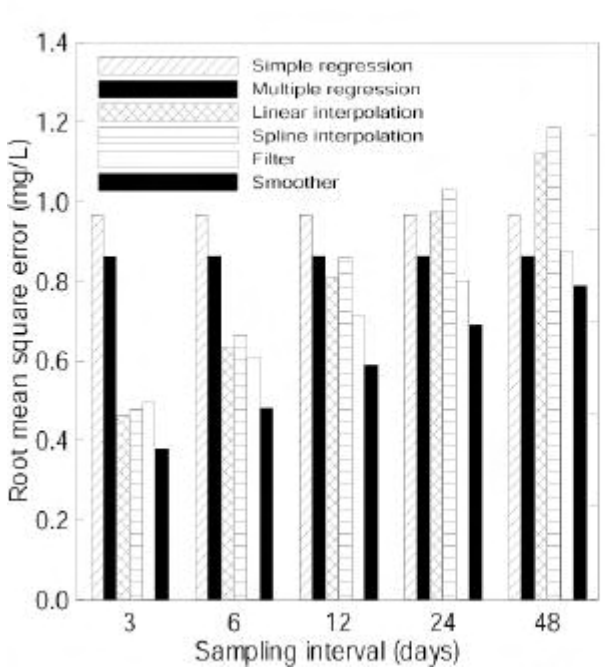

Figure 3. Average root-mean-square error of selected estimators for specified sampling intervals

SUMMARY

This paper develops optimal estimators for on-line and off-line computation of suspended-sediment concentrations in streams and compares the accuracies of the optimal estimators with results produced by interpolators and regression estimators. The analysis uses long-term daily-mean suspended-sediment concentration and streamflow data from ten sites within the United States to compare accuracies of the estimators. A log transformation was applied to both suspended-sediment concentration and streamflow values prior to development of the estimates.

The optimal estimators are based on a Kalman filter and an associated smoother to produce the on-line and off-line estimates, respectively. The optimal estimators included site-specific parameters, which were estimated by generalized least squares, to account for influences associated with ancillary variables, including streamflow and annual seasonality, on suspended-sediment concentrations. In addition, the optimal estimators account for autoregressive-error components and uncertainties in the accuracy of direct measurements in computing continuous records of suspended-sediment concentrations. Results were compared with estimates produced by both linear and cubic-spline interpolators, which do not account for ancillary variables, and with simple and multiple-regression estimators, which do not locally account for the suspended-sediment concentration measurements.

The average standard error of simple and multiple regression estimates was 124 and 105 percent, respectively. The accuracies of interpolators, and on-line and off-line estimators are related to measurement frequency, and were compared at simulated measurement intervals of 3, 6, 12, 24, and 48-days. The average standard error of the linear interpolator ranged from 48.4 percent for 3-day sampling intervals to 159 percent for 48-day sampling intervals. The average standard error of the cubic spline interpolator ranged from 50.6 percent for 3-day sampling intervals to 176 percent for 48-day sampling intervals. The average standard error for the on-line estimator ranged from 52.7 percent for a 3-day sampling interval to 107 percent for 48-day sampling interval. The average standard error of the off-line estimator ranged from 39.9 percent for a 3-day sampling interval to 93.0 percent for a 48-day sampling.

The use of the optimal estimators rather than interpolators or regression estimators will improve the accuracy and quantify the uncertainty of records computed on the basis of suspended-sediment concentrations measured at intervals less than 48 days. Although in this paper, parameters for the estimators were developed on the basis of daily values data, it is anticipated that in typical applications the estimators will be development on the basis of unit-value data and direct measurement information.

REFERENCES CITED

Bukaveckas, PA, Likens GE, Winter TC, Buso DC. 1998. A comparison of methods for deriving solute flux rates using long-term data from streams in the Mirror Lake watershed. Water, Air, and Soil Pollution 105: 277-293.

Burkham DE. 1985. An approach for appraising the accuracy of suspended-sediment data. U.S. Geological Survey Professional Paper 1333; 18.

Ferguson, RI. 1986. River loads underestimated by rating curves. Water Resources Research 22: (1): 74-76.

Gelb A(Ed.). 1974. In Applied Optimal Estimation, M.I.T. Press: Massachusetts Institute of Technology, Cambridge, Massachusetts; 374.

Grewal MS, Andrews AP. 1993. In Kalman Filtering--Theory and Practice, Prentice Hall Information and System Science Series: Englewood Cliffs, New Jersey; 38

Helsel DR, Hirsch RM. 1992. Statistical Methods in Water Resources. Studies in Environmental Science 49: Elsevier, New York; 522.

Koltun GF, Gray JR, McElhone TJ. 1994. User's manual for SEDCALC, A computer program for computation of suspended-sediment discharge. U.S. Geological Survey Open-File Report 94-459; 46.

Phillips JM, Webb BW, Walling DE, Leeks GJL. 1999. Estimating the suspended sediment loads of rivers in the LOIS study area using infrequent samples. Hydrological Processes 13: (7): 1035-1050.

Siouris GM. 1996. In Optimal control and estimation theory: John Wiley: New York; 407.

Walling DE, Webb BW. 1988. The reliability of rating curve estimates of suspended sediment yield; some further comments. In, Bordas MP, Walling DE (editors). 1988. Sediment Budgets, International Association of Hydrological Sciences (IAHS)-AISH Publication 174, Meeting in Porto Alegre, Brazil; 350.

Yang, CT. 1996. In Sediment Transport -- Theory and Practice, McGraw-Hill: New York; 396.

DATA MINING AND CALIBRATION OF SEDIMENT TRANSPORT MODELS

Peter Waldo, Geologist, USDA NRCS, Fort Worth, TX

INTRODUCTION

Data mining consists of the discovery of patterns and trends in data sets to find useful decision-making relationships. This study illustrates the application of statistical data mining techniques to hydrologic and sediment data from 6 stream gaging stations in the Susitna River basin, Alaska (Williams and Rosgen, 1989). The Susitna River basin occupies more than 50,000 km^2 in southcentral Alaska. Brabets (1996) described stream flow hydrology in southcentral Alaska and Knott, et. al. (1987) developed predictive equations of suspended sediment and bedload discharges for the stations in the Susitna basin. The 6 stations are listed in Table 1.

Table 1. Selected stations in Susitna River basin, Alaska.

USGS Station (Symbol)	Location (Correspondence Class)[1]	Drainage Area, km^2	Area Covered by Glaciers, %[2]
15292100 (ST)	Susitna near Talkeetna (1)	16,368	7
15292400 (C)	Chulitna below Canyon (2)	6,656	27
15292439/40 (SC)	Susitna below Chulitna (4)	23,179	--
15292700 (T)	Talkeetna (3)	5,195	5
15292780 (SS)	Susitna at Sunshine (4)	28,747	--
15294345 (Y)	Yentna (4)	16,005	--

1 Correspondence class groups stations by similarity in geomorphic, hydraulic, and sediment properties. 2 Knott et al., 1987.

The purpose here is to improve understanding of the data by examining their structure through statistical data mining techniques. The data structure is then related to prior knowledge or theories of geomorphology, hydrology, or sediment transport. The proposed relationships are formulated as hypotheses and tested by the methods of statistical inference.

The data may be visualized as a matrix with n rows and p columns. Each column represents a variable, some of which are continuous (e.g., water discharge) and others are descriptive (e.g., gaging station names). The rows represent the observations and measurements made on a given date at a given gaging station. Data mining looks for structure or patterns of association within the n x p matrix. Factor analysis finds relationships among the continuous variables (Stevens, 1992; Waldo, 1998; 2000a). Cluster analysis formulates hypothetical groupings of similar cases or rows. The resulting patterns are interpreted by graphical methods, contingency tables, correspondence analysis, and regression.

The Susitna data (Williams and Rosgen, 1989) contains 187 cases and 73 reported and derived variables. Each continuous variable was transformed to an approximately normal distribution by power transformations (Velleman, 1988; Waldo, 1998; 2000a). Symbols of the variables reported in this manuscript are A = drainage area, km^2; Q = water discharge, m^3/s; V = velocity, m/s; W = channel width at level of water surface, m; D = flow depth, m; T = temperature, ºC; C = suspended sediment concentration, mg/l; S = suspended load, kg/s, or suspended sediment property; B = bedload, kg/s, or bedload sediment property; and M = bed material property. Subscripts denoting sediment properties are sd = sand, %; cb = cobbles, %; d50 = median grain size, mm. The natural logarithm is used in some transformations and is designated by ln.

FACTOR ANALYSIS

Factor analysis in this study consists of principal components analysis of the correlation matrix with varimax rotation. Factor analysis applies to the continuous variables which occupy 69 of the 73 columns in the Susitna data base. The large number of variables relative to the number of cases (N = 187) causes problems with interpreting results. The following strategy was employed in this study.

Combine the variables into 4 groups based on the type of information they convey: (1) geomorphic, sediment load, and hydraulic variables; (2) suspended sediment variables; (3) bedload sediment variables; (4) bed material variables. Factor analysis is performed separately on each of the 4 groups of variables. See Table 2 for an example. Select a subset of variables to represent each of the 4 groups based on the significance and patterns of the variable loadings on the factors (Stevens, 1992).

Table 2. Factor analysis of bedload variables (N = 182).

Variable	Factor 1 (Medium)	Factor 2 (Fine)	Factor 3 (Coarse)	Communality
B, kg/s	-.60			.45
<0.062 mm		-.66		.44
<0.12 mm		-.83		.70
<0.25 mm		-.67		.45
<0.5 mm	.85			.76
< 1 mm	.98			.96
< 2 mm	.98			.98
< 4 mm	.97			.97
< 8 mm	.95			.97
< 16 mm	.87		.39	.92
< 32 mm	.65		.58	.78
< 64 mm			.83	.69
Sand %	.98			.98
Gravel %	-.99			.98
Cobbles %			-.82	.69
d_{min}, mm		.68		.47
d_{50}, mm	-.72			.62
d_{max}, mm	-.62		-.49	.64

Note: Only loadings judged significant at $\alpha = 0.01$ are shown. Variables selected to represent the bedload subset of variables in other multivariate analyses are designated by bold type.

Combine the 4 subsets of variables into a new matrix. Perform factor analysis on that matrix and use the results to represent the multivariate interactions of the original 69 continuous variables. Examine the results (Table 3) and formulate hypotheses or theories about the loading patterns of the variables on the factors.

Table 3 contains the final results of factor analysis of the Susitna River data. Note that N = 146 and not 187 because of missing measurements from 41 cases. Factor 1 expresses sediment transport characteristics of the data whereas factor 2 expresses hydraulic roughness. Factor 3 characterizes geomorphic attributes of the watersheds above the gaging stations and factor 4 conveys information about fluid properties of the stream water.

Communality (Tables 2 and 3) designates the degree of variance of a given variable accounted for by the chosen factors. Suspended sediment load (S) and bedload (B) are candidate dependent variables for which predictive equations might be desired. The 16 variable-4 factor analysis in Table 3 accounts for about 91% of the variance of S but only about 75% of the variance of B. This suggests that a predictive model of S might be calibrated more successfully from these data than for B. The lower communality of B might be accounted for by a greater degree of randomness, elimination of one or more key predictors in the data reduction analysis (Table 2), or failure to include appropriate data in the original matrix (e.g., stream bank properties).

The factor analysis can be used to select a candidate predictor set for regression analysis. For example, the dependent variable B loads significantly on both factors 1 and 2 (Table 3) and one or more predictors should be selected from each factor. In factor 1 B_{sd} and B_{d50} should not be included because they are properties of the bedload itself. C and S should be excluded because they will be considered as dependent variables in other regression calibrations. Q, V and D are potential candidates for the predictor set and from factor 2 the 3 properties of the bed

material (M) could also be included. The subset of 6 variables can be further reduced by screening analysis (SAS Institute, 1995) or by the reduced model-full model (RM-FM) test (Neter, et. al., 1990; Waldo, 1998, 2000b).

Table 3. Factor analysis of selected variables, Susitna River, Alaska (N = 146).

Variable	Factor 1 (Sediment)	Factor 2 (Roughness)	Factor 3 (Geomorphology)	Factor 4 (Fluid)	Communality
$A^{0.5}$			-.93		.90
$Q^{0.33}$	-.48		-.84		.98
$V^{1.25}$	-.67	.43			.72
ln W			-.93		.87
$D^{0.67}$	-.68				.68
T				-.66	.52
$C^{0.17}$	-.75			-.43	.81
$S^{0.125}$	-.71		-.50		.91
$B^{0.25}$	-.67	-.54			.75
$S_{sd}^{0.6}$				.90	.87
ln S_{d50}				.89	.84
$B_{sd}^{1.67}$	.93				.87
$B_{d50}^{-0.67}$	.88				.82
$M_{sd}^{0.4}$		-.90			.82
$M_{cb}^{0.67}$		.92			.87
$M_{d50}^{0.75}$		.96			.95

Loadings of variables considered insignificant at $\alpha = 0.01$ are not shown.

Factor scores may be saved as variables and used in other statistical techniques such as regression and cluster analysis. They provide a means for determining the success of normalizing transforms of the original variables (Waldo, 2000a). Factor scores may be used to correlate other variables to the factors. For example, slope of the water surface was not reported (Williams and Rosgen, 1989) for 2 of the 6 stations. Correlations of slope to the factor scores suggest it relates primarily to watershed geomorphology variables as follows:

Factor 1 (Sediment Transport):	-0.26
Factor 2 (Hydraulic Roughness):	0.19
Factor 3 (Geomorphology):	-0.80
Factor 4 (Fluid Properties):	-0.31

CLUSTER, CONTINGENCY TABLE, AND CORRESPONDENCE ANALYSES

Cluster analysis includes a variety of techniques used for exploring data structure (Massart and Kaufman, 1983; Waldo, 1998). The method chosen for this study consists of hierarchical clustering of cases by Ward's method. Cluster analysis may reveal several levels of structure in the data (Waldo, 1998) and the level most relevant to the purposes of this study is selected by interpretation (Figure 1a). The variables used to characterize the structure of the cases were the 16 variables selected by factor analysis (Table 3).

Four clusters were selected to interpret data structure. The geomorphological relevance of each cluster may be inferred by comparing mean values of the variables in the cluster to those of the other 3 clusters (Figure 1b). For example, the Type 3 cluster has relatively low discharges of water and sediment compared to the other clusters. The texture of suspended, bedload, and bed material sediments is sandy compared to the other clusters. The nature of the Type 3 cluster suggests it represents lower flows carrying limited amounts of sandy sediments. Other cluster types may be interpreted in a similar manner.

Each case used in the analysis may be classified according to cluster type (SAS Institute, 1995). The relationship of the nominal values of cluster type to other descriptive variables can be investigated by contingency tables and correspondence analysis. The potential relationship of cluster type to stream gaging station is of interest here.

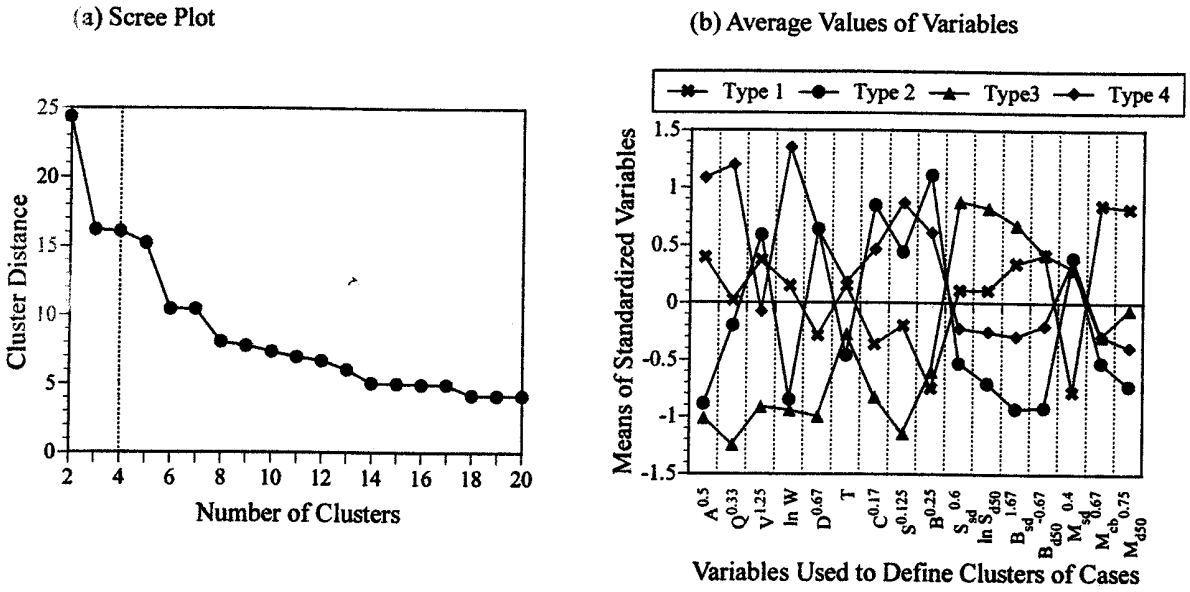

Figure 1. Types of stream station data derived from hierarchical cluster analysis of 16 variables and 165 cases, Susitna River basin, Alaska. (a) Scree plot, showing that 4 clusters is 1 possible interpretation of the clustering results. (b) Average values of variables by cluster. Type 1 = low bedload transport, moderate suspended sediment discharge, armoured bed; Type 2 = moderate water and high sediment discharges in smaller watershed indicative of glacial meltwater; Type 3 = low discharges of water and sediment from smaller watershed, sandy sediment of limited supply; Type 4 = larger watersheds with substantial water and sediment discharges, sandy bed material.

Contingency table analysis produces a statistic known as the uniformity coefficient, $R^2(U)$, that indicates the degree of association between two descriptive variables. The value of $R^2(U) = 0.70$ (Figure 2a) indicates a high degree of association between cluster type and gaging station. Correspondence analysis shows which stations associate more strongly with which cluster type (Figure 2b).

The 6 stations may be grouped into 4 classes depending on their correspondence to cluster type (Table 1). This associates cluster type, originally determined from 165 cases, with all 187 cases. Missing values of underrepresented variables (e.g., water surface slope) can be predicted by computing means or medians of the variables for each cluster type or correspondence class. Either cluster type or correspondence class may be used to define indicator variables for use in regression analysis. The significance of differences between types or stations in various model spaces can be assessed by statistical hypothesis tests.

REGRESSION ANALYSIS

Regression analysis is typically used in sediment transport studies for calibrating predictive models. Suspended sediment and bedload discharges are regressed on water discharge or other predictors. Calibrations are performed separately at each station (Knott, et. al., 1987). When data are sparse at certain stations (e.g., Susitna River at Chulitna River and Yentna River, Table 4) the significance of calibrations is suspect because of low statistical power (Waldo, 2000b).

An alternative strategy consists of using regression in the data mining approach. Select the dependent variables for which predictive models are to be developed (e.g., suspended sediment and bedload discharges). Assure that those variables are included in the factor and cluster analysis steps of the data mining procedure. Select candidate predictor variables from factor analysis. Use the results of cluster and correspondence analysis to define convenient yet meaningful groups. Include indicator variables representing the descriptive groups in the predictor set. Appropriate indicator variables and their interactions with the continuous predictors can significantly increase R^2

and reduce mean square error (MSE) of the models especially when optimal models are derived from the RM-FM test (Neter et. al., 1990; Waldo, 1998; 2000b). The resulting calibrations test the significance of decisions made previously in factor and cluster analysis and identify predictor sets for the final calibration of predictive models.

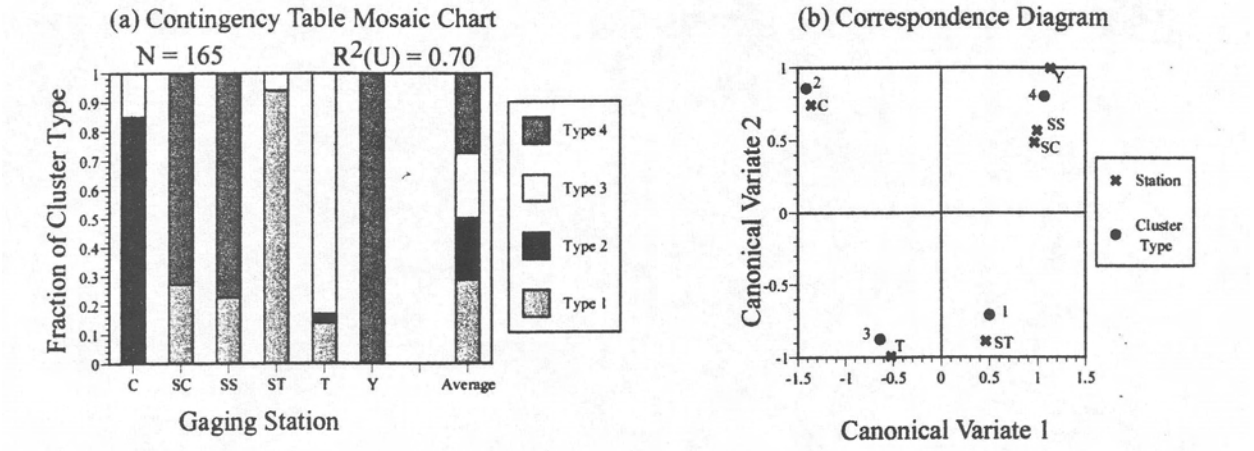

Figure 2. Correspondence of 4 hierarchical cluster types to 6 gaging stations in the Susitna River basin, Alaska. C = Chulitna River; SC = Susitna River below Chulitna River confluence; SS = Susitna River at Sunshine; ST = Susitna River near Talkeetna; T = Talkeetna River at Talkeetna; Y = Yentna River. Cluster Type 1 = armoured bed, low sediment lead; 2 = unarmoured bed, high sediment load; 3 = low sediment load, sandy sediment; 4 = larger watersheds, high sediment load.

Table 4 reports model calibrations for suspended load and bedload discharges regressed on the continuous predictor water discharge. Logarithmic transforms were used for all continuous variables because the logarithms performed as well or better in the regressions than the univariate normalizing power transformations used in factor and cluster analysis. Some calibrations to individual stations suffered from low R^2, high MSE, low transportability to other data as indicated by R^2_{PRESS}, and are of questionable significance because of low N. A coefficient calibrated individually at one station cannot be statistically compared to the coefficients at the other stations.

Suspended load and bedload discharges were calibrated to water discharge using 5 indicator variables identifying the 6 stations (see the grouping variable "stations" on Table 4). Another model using 3 indicators to represent correspondence class was also calibrated (Figure 3; Table 4). Validation statistics indicate the models for class are nearly as good as the models using indicators for the stations (Table 4). The use of 3 indicators to define correspondence class as a grouping variable as opposed to 5 indicators to define stations does not increase modeling efficiency much in this example. However, if more stations were included in the data set defining indicators based on correspondence class would lead to a full model predictor set containing far fewer predictors.

Inspection of Figure 3 reveals 2 limitations of the linear models representing the 4 correspondence classes. First, some of the linear segments fit their respective classes somewhat poorly suggesting nonlinearity in the models. Second, the 4 classes could be combined into 2 broader groups. For example, the classes designated "Armoured Bed" and "Mixed Channel Type" in Figure 2a could be combined into 1 group and a nonlinear model fit to those data. Nonlinearity may be investigated by including polynomials of the continuous predictor lnQ in the model and testing their significance.

The viability of using 2 groups of stations was tested by defining the groups by graphical methods (SAS Institute, 1995; Velleman, 1997). The data were plotted by station on lnS and lnB v. lnQ scatterplots. The 6 stations (i.e., 4 correspondence classes) were combined into 2 slightly different groups on the lnS and lnB plots. For example, the classes "Abundant Sediment Supply" and "Limited Sediment Supply" (Figure 3) correspond to the stations on Chulitna and Talkeetna Rivers respectively (Figure 2b). The data plot on nearly the same trend, suggesting they can be grouped together. Chulitna River tends to have higher water and sediment discharges than Talkeetna River although both have similar drainage areas because a higher percentage of the Chulitna headwater area is covered by

glaciers (Table 1; Knott et al. 1987). The two visual groups seem to highlight differences in sediment transport between stations on tributaries and stations on the main stem of the Susitna River.

Table 4. Model calibrations, Susitna River, Alaska.

Grouping Variable	N	p	R^2	MSE	R^2_{PRESS}	p--value
			Suspended Load			
C	43	1	.913	.098	.900	<.0001
SC	11	1	.752	.427	.628	.0005
SS	42	1	.869	.141	.854	<.0001
ST	39	1	.900	.188	.886	<.0001
T	42	1	.860	.275	.846	<.0001
Y	10	1	.810	.121	.719	.0004
Stations	187	7	.924	.182	.917	<.0001
Class[1]	187	5	.922	.186	.916	<.0001
			Bedload			
C	43	1	.154	.230	.055	.0094
SC	11	1	.310	.457	--[2]	.0753
SS	42	1	.185	.405	.119	.0045
ST	39	1	.754	.294	.716	<.0001
T	42	1	.519	.556	.460	<.0001
Y	10	1	.012	.124	--[2]	.7659
Stations	187	7	.830	.363	.812	<.0001
Class[1]	187	6	.799	.427	.780	<.0001

N = number of observations; p = number of predictors; R^2 = coefficient of determination; MSE = mean square error; R^2_{PRESS} = R^2 computed from Press statistic; p-value from ANOVA table for the regression.

1 Class determined by correspondence of 6 stations to 4 cluster types. 2 R^2_{PRESS} is undefined because Press statistic > total sum of squares.

Regression analysis and the RM-FM test are useful for screening the significance of continuous predictors other than Q. Selections of candidate predictors were made by factor analysis. Models for lnS and lnB were obtained using an indicator based on the 2 groups identified by the visual method. Suspended sediment was found to be sensitive to lnD in addition to lnQ and M_{d50} enhanced the calibration of the bedload model. Polynomial terms of the continuous predictors and their interactions with the indicator variable and each other were included in the full models. This resulted in linear models, an assumption important to least squares regression (Figure 4). The suspended sediment model has normally distributed residuals with constant variance but exhibit a significant degree of dependence (Figure 4a). The bedload model has normally distributed independent residuals but with nonconstant variance (Figure 4b). This suggests the type of generalized least squares to use in the final calibrations of the models: correction of serial correlation of the suspended sediment model and weighted least squares to correct nonconstant variance in the bedload model.

CONCLUSIONS

1. Data mining leads to a sophisticated understanding of data structure. Knowledge of data structure improves theoretical understanding of the data and enables calibration of reliable predictive models. The data mining methodology enables efficient use of existing data in addressing specific problems (e.g., sediment transport

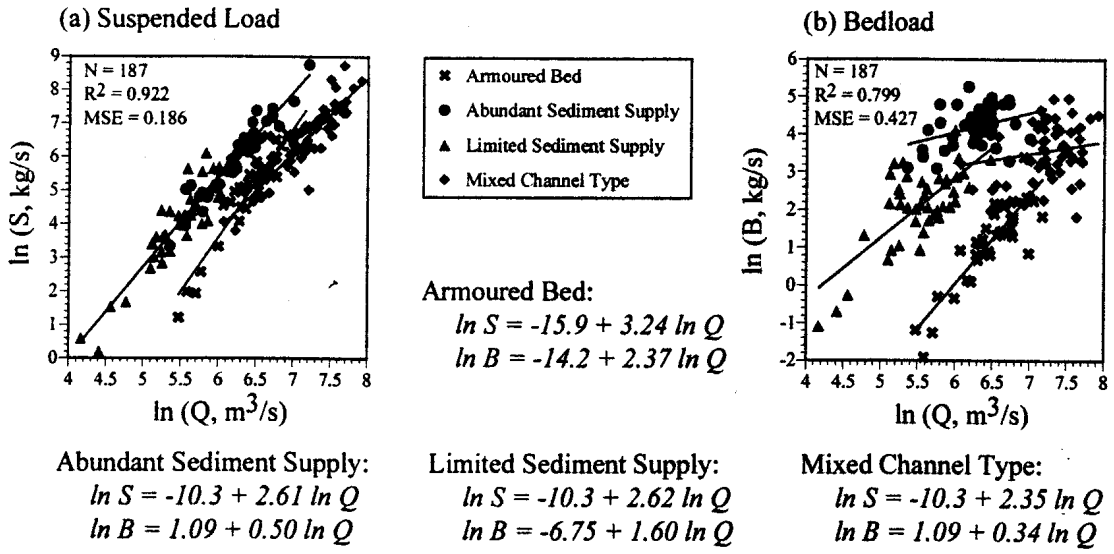

Figure 3. Relationship of (a) suspended load and (b) bedload to water discharge, Susitna River basin, Alaska. Data from 6 gaging stations are grouped into 4 classes by correspondence analysis of the stations to 4 cluster types determined by hierarchical clustering. Models calibrated by the reduced model-full model test using ordinary least squares.

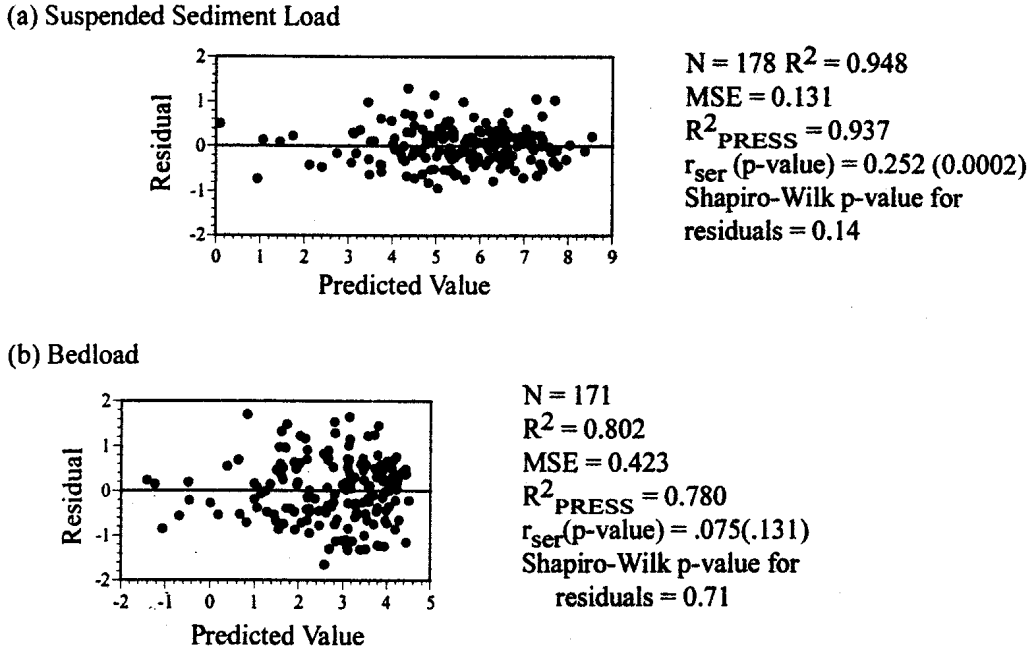

Figure 4. Diagnostics for multivariate models of sediment loads, Susitna River basin, Alaska. Residuals and predicted values are in units of ln S and ln B both of which are originally in units of kg/s. Vertical and horizontal scales in both graphs are identical. (a) Suspended sediment load, with 3 missing cases and 5 outliers removed. Predictor set includes cubic polynomials of ln Q and ln D, an indicator grouping the 6 gaging stations into 2 sets, and selected interaction terms. (b) Bedload, with Yentna data and 6 outliers removed. Predictor set includes cubic polynomials of ln Q and M_{d50}, an indicator grouping the 6 gaging stations into 2 sets, and selected interaction terms.

predictions). This approach might be used in the development of data collecting strategies to optimize results of future experiments.

2. Factor analysis finds meaningful groups of continuous variables, reduces the number of variables needed in subsequent analyses, suggests candidates to include in regression predictor sets, and produces factor scores useful for validating other statistical procedures.

3. Cluster analysis and graphical methods define groups of cases that can be interpreted in a manner that increases understanding of the data structure. Indicator variables may be defined on the basis of cluster type and tested for significance by regression analysis.

4. Contingency tables and correspondence analysis relate cluster types to gaging stations. This enhances understanding and interpretation of the data structure and facilitates model calibration.

5. Regression analysis with the RM-FM test evaluates hypotheses about the data structure, investigates potential predictor sets for model calibration, and suggests methods needed to calibrate the final model as efficiently and accurately as possible.

6. The data structure reflects geomorphic attributes of the Susitna River basin as well as hydraulic and sedimentologic relationships. Data mining methods enable incorporation of that information into model calibrations through the use of indicator variables and the process of identifying key predictor variables.

REFERENCES

Brabets, T.P., 1996, Evaluation of the streamflow-gaging network of Alaska in providing regional streamflow information, Water-resources investigation report 96-4001, USGS, Anchorage, Alaska.

Knott, J. M., Lipscomb, S. W., Lewis, T. W., 1987, Sediment transport characteristics of selected streams in the Susitna River basin, Alaska: Data for water year 1985 and trends in bedload discharge, 1981-85, USGS open-file report.

Massart, D. L., Kaufman, L., 1983, The interpretation of analytical chemical data by the use of cluster analysis, John Wiley and Sons, New York.

Neter, J., Wasserman, W., Kutner, M. H., 1990, Applied linear statistical models, Irwin, Boston.

SAS Institute, 1995, JMP statistics and graphics guide, SAS Institute, Cary, North Carolina.

Stevens, J., 1992, Applied multivariate statistics for the social sciences, Lawrence Erlbaum, Hillsdale, New Jersey.

Velleman, P. F., 1997, Data desk version 6.0 statistics guide, Data Description Inc., New York.

Waldo, P. G., 1998, Prediction of sealing capacity of faults: a pilot study using observational statistics, Ph.D. dissertation, Univ. Tex. at Arlington, Arlington, Texas.

Waldo, P. G., 2000a, Factor analysis and hydrologic data from Texas, manuscript in preparation.

Waldo, P. G., 2000b, Selecting optimal regression models by the reduced model-full model test, manuscript in preparation.

Williams, G. P., Rosgen, D. L., 1989, Measured total sediment loads (suspended loads and bedloads) for 93 United States streams, USGS open-file report.

A Probabilistic Approach To Modeling Erosion for Spatially-Varied Conditions

W. J. Elliot **P. R. Robichaud** **C. D. Pannkuk**
Project Leader **Research Engineer** **Soil Scientist**
USDA-FOREST SERVICE, ROCKY MOUNTAIN RESEARCH STATION
Moscow, ID 83843

Mailing address: 1221 South Main, Moscow, ID 83843; Tel. 208 882 3557; email welliot@fs.fed.us

INTRODUCTION

Soil erosion by water is a complex process resulting from the interactions among a number of factors including weather patterns, soil properties, topography, and the influences of surface vegetation. Natural variability is a dominant characteristic of each of these factors, which makes predicting soil erosion rates difficult. In many forest conditions, and some rangeland conditions, erosion may be minimal under vegetated conditions unless the site is disturbed. Disturbances may be fire, logging, grazing, or severe precipitation events. The most extreme erosion rates occur when severe weather follows a major disturbance, particularly a severe wildfire.

Natural resource managers need tools to aid in predicting soil erosion following wildfires to estimate potential loss of onsite productivity, or potential offsite damage from sediment to aquatic ecosystems or other beneficial uses dependent on quality water. Current erosion prediction tools generally are developed from agricultural erosion models, which are intended to provide long-term estimates of soil erosion rather than evaluate short-term risks. These models typically provide an "average" erosion value, and do not give any estimate of the likelihood of major upland erosion occurring.

Process-based erosion models may provide a means for evaluating complex distributions of disturbance from a range of possible weather sequences, but the effort to parameterize such models makes them unsuitable for widespread application. However, they can play a role in assisting researchers to analyze some of the interactions between erosion factors.

We are developing an interface to aid in the analysis of erosion prediction following fire, or a similar major disturbance, in forests and rangelands. This paper addresses how we intend to incorporate the inherent variability associated with the predicted erosion rate, and how that variability is influenced by weather, spatial distribution of disturbances, and soil properties.

POST-FIRE EROSION FACTORS

Hillsides are more susceptible to erosion following a fire with decreased canopy and surface residue, and in some case a soil that is water repellent. Water repellency is a process that occurs when volatilized hydrocarbons released by the fire condense and coat soil particles and aggregates. These hydrocarbons repel water, which reduces infiltration rates and increases runoff, erosion and sediment delivery from hillsides. With time, they are dissolved by

infiltrating water from rainfall and snowmelt. The reduction in vegetative canopy and surface residue dramatically increases the potential for soil erosion by increasing the area susceptible to raindrop impact and decreasing the potential for sediment deposition. In the year following a fire, vegetation regrowth can be rapid because of increased availability of soil nutrients, and decreased competition for sunlight and soil water by large trees. Hence, a burned site has a far greater likelihood of erosion the year following a fire, with the risk dropping rapidly as vegetation regrows, residue accumulates, and water-repellent chemicals break down and are flushed from or translocated in the soil.

VARIABILITY IN SOIL EROSION

Variability has been identified as a dominant feature in soil erosion research. Coefficients of variations and confidence intervals are the most familiar ways of reporting uncertainty, but typically they are used only for comparisons. The concept of confidence intervals can be extended to a complete probability distribution, which can describe a range of values, each value with an associated probability of occurrence.

Weather Weather is highly variable from one year to the next. Years with a wet spring, encouraging considerable vegetation growth, followed by a prolonged, hot summer are more likely to have severe rangeland wild fires than are years with drier springs, or cooler or wetter summers. In forests, low snow pack years with hot dry springs and summers are more likely to have severe wild fires.

Following a fire, if the weather is very dry, there will be little natural or seeded vegetation regrowth and little soil recovery from water repellent conditions. This means that the site can remain susceptible to erosion for another season. If the weather is very wet, and the soils are water repellent, there is a high likelihood of severe soil erosion, but also there will be rapid vegetation recovery. Runoff from rainfall or rain-on-snow events will be much greater than runoff from melting snow. Generally, snowmelt rates are 1 to 2 mm hr^{-1}, whereas rainfall rates up to 25 mm hr^{-1} are common.

Once a site has recovered, rainfall rates in excess of 50 mm hr^{-1} or total rainfall amounts greater than 100 mm within a day or two are necessary before any significant upland erosion will occur. This seldom happens in many forested areas.

Fire Fire effects on erosion are not homogenous. Fire severity is a description of the impact of a fire on the soil and its litter layer. The severity of a fire varies widely in space, depending on fuel load, moisture conditions and weather at the time of fire, and the topography. This variability often creates variability in severity, leading to mosaic landscapes. Areas that are drier, such as those near ridge tops, and areas with greater amounts of fuel, may experience higher severity fires. Areas that are wetter, such as riparian areas, will likely have less severe fires (Robichaud and Miller 2000).

Soil and Spatial Variability Soil properties are naturally highly variable. Soil erosion experiments generally measure standard deviations in erodibility values similar to the means, and

coefficients of variation greater than 30 percent are common (Elliot et al. 1989). Soils near the tops of ridges tend to be coarser grained and shallower, whereas soils at the bottoms of hill slopes may be finer grained, while flood plains vary widely depending on past geomorphic processes. After fires, this variability increases with variability in water repellency.

The combined effects of a mosaic in fire severity and soil variability result in spatial variability of soil erodibility that has some degree of predictability, but a great deal of natural variability. Spatial variability analyses have shown that following some fires, there are definite trends in degree of fire severity, whereas, the variability is evenly distributed on a hillslope or watershed following other fires (Robichaud and Miller 2000).

COMBINING VARIABILITIES

To understand the combined variabilities of climate, fire severity, and soil properties, numerous analyses are carried out combining various storms or weather patterns, different distributions of disturbance, and an array of soil properties that occur for a given severity of fire. It is unreasonable to expect that a single estimate of soil erosion will capture the combined probabilities. A better estimate of erosion is to provide a range of possible erosion predictions using a Monte-Carlo approach (Haan 1994). The estimated erosion rate can then be expressed as the probability of a given level of erosion being exceeded. One of the challenges for this type of modeling is developing the statistical distributions of the dependent variables.

THE WEPP MODEL

We chose to use the Water Erosion Prediction Project (WEPP) model as the driver for the proposed model. WEPP is a physically-based soil erosion model that describes the processes that cause erosion (Laflen et al. 1997). As long as the processes are correctly described, and the details of the site conditions can be described by the input variables, then the model can be applied. For some runs, WEPP may require up to 400 input variables describing soil and vegetative properties in great detail. Packaged with WEPP is a daily weather generator, CLIGEN. CLIGEN stochastically generates daily weather sequences, which include the occurrence of precipitation, and the amount and duration of precipitation on a wet day (Nicks et al. 1995).

The WEPP model can be run either for single storms, with initial conditions such as soil water content, surface cover and soil erodibility specified for the storm, or in continuous mode where these values are automatically altered daily for a number of years of daily weather. Output options from WEPP include average annual runoff and erosion rates, annual erosion rates for the length of run, or event runoff and erosion rates for every runoff event during the period of simulation (Flanagan and Livingston 1995). The WEPP model has been applied to forest conditions with reasonable results, and the database to support the model is increasing (Elliot and Hall 1997).

PROPOSED SPATIALLY-VARIED MODEL

We are developing a soil erosion interface to use with the WEPP model, combined with a

Table 1. Range of erodibility values observed in field studies.

Fire Severity	Remaining Ground Cover (percent)	Saturated hydraulic conductivity (mm hr^{-1})	Rill erodibility ($s\ m^{-1}$)
Low	40 – 100	12 – 30	$3 \times 10^{-5} – 3 \times 10^{-4}$
High	0 – 60	6 – 15	$2.5 \times 10^{-4} – 2.5 \times 10^{-3}$

stochastic input data set, to estimate the probability of a given level of soil erosion (Robichaud et al. 2000). The user will provide inputs related to local climate, degree of fire severity, soil texture, and topography. The user will be given the option to use a storm generated by the interface, or to specify the desired storm amount and duration. Once the storm is selected, the proposed interface will be run for a large number of spatial distributions and soil property combinations, producing a range of possible soil erosion rates. The results will be presented to the user in either a tabular or a graphical format.

Climate There are few weather stations in remote forested areas, a weather station some distance from the site of concern may not provide an adequate estimate for a storm. The CLIGEN weather generator has a database of over 1100 stations (Flanagan and Livingston 1995). We have expanded that database to over 2600 (Scheele et al. 2001). In addition, we have access to the PRISM database that contains monthly precipitation values for a 4 km grid covering the entire continental U.S. This grid will aid users to select a local climate for the CLIGEN weather generator (Scheele et al. 2001). CLIGEN can then generate a long term climate for running WEPP. To estimate the risk of a given size of storm, a 100-year climate file will be generated to run WEPP. WEPP will be run and the output for each event will be requested. The event output file will be sorted to determine the greatest, second greatest, fifth, tenth, and twentieth greatest erosion events. The storms for these events will provide the user with a choice of 5-, 10-, 20-, 50-, and 100-year return periods for storms. The user can select the desired return period storm, or specify a storm.

Soil Research has shown that it is not possible to statistically differentiate more than two levels of fire severity, which we define as low and high (Robichaud et al. 1993). The most important erosion prediction parameters affected by fire severity include percent ground cover, saturated hydraulic conductivity, and rill erodibility. Table 1 presents the range of values that have been measured in field studies. These values can be adjusted for different textures based on research observations (Robichaud 2000).

Spatial Spatial variability can be described with different distributions of severity on the landscape (figure 1). Figure 1 shows that the distributions can be grouped into categories of erosion risk. Most managers prefer to describe burned sites by these categories of erosion risk as "High", "Moderate" or "Low". In a previous study, Robichaud and Monroe (1997) showed that dividing the hill into three elements is adequate to describe the range of variation of surface erosion as influenced by spatial variation.

RESULTS

Climate Variability Table 2 presents the results of a set of WEPP runs comparing different storm events for a forest with a moderate erosion risk fire. Note that the events that experienced

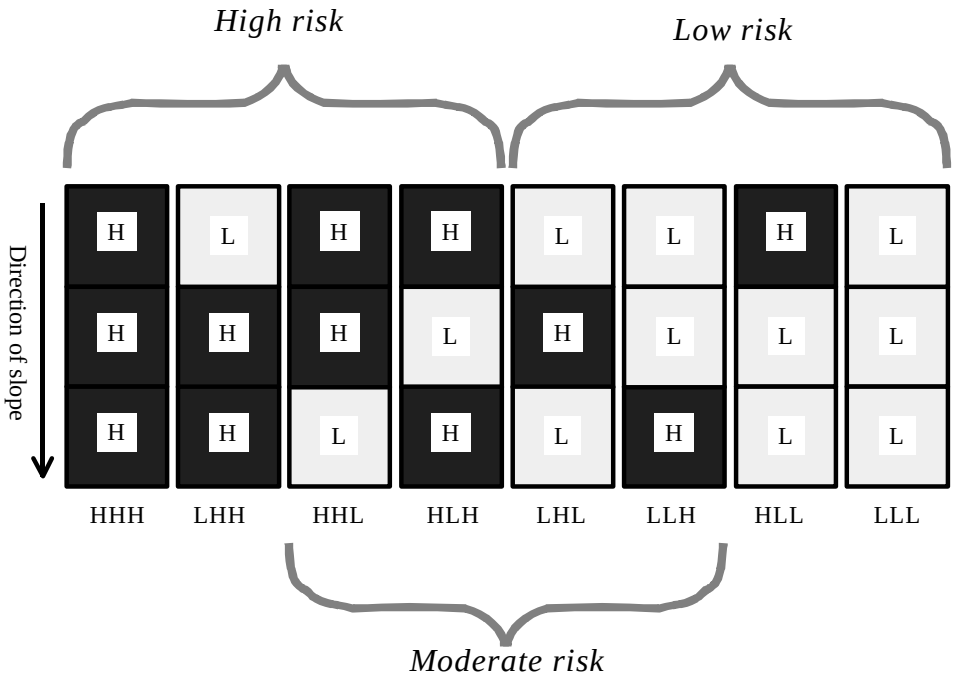

Figure 1. Spatial distributions of high (H) and low (L) fire severity describing low, moderate, and high erosion risk.

the greatest erosion were not from the largest storms. Some of the largest storms occurred as snowfall, while it is likely that most of the events that caused the greatest amounts of erosion and sediment delivery were from rainfall on a snowpack. Table 2 also shows that the CLIGEN storms were similar to the 6-hr storms predicted by the NOAA atlas (1973) for central Idaho. Work is ongoing to alter the random number generators within CLIGEN, which will likely alter the magnitudes of the largest storms (Flanagan et al. 2001).

Spatial Variability Single sets of soil properties were defined for low and high severity, and a set of WEPP runs were carried out with the soil properties fixed to demonstrate the variability that can be modeled simply by altering the spatial distribution of the fire severity on the hillside (figure 1). Table 3 presents the results of this analysis for a 6-hr storm producing 60 mm of

Table 2. Summary of events for a severely eroded hillslope from a 100-year WEPP run, with the Warren, ID climate, a slope length of 300 m, and a slope steepness of about 40 percent.

	By Detachment			By Delivery			By Precipitation			
Event	Date	**Detachment**	Precip	Date	**Delivery**	Precip	**Precip (mm)**		Date	Delivery
	(m/d)	**(Mg ha^{-1})**	(mm)	(m/d)	**(Mg ha^{-1})**	(mm)	NOAA 6-h	CLIGEN	(m/d)	(Mg ha^{-1})
Largest	3/30	**97.5**	35.3	4/28	**3.39**	15.0	53.3	**64.7**	3/4	0.00
2nd Largest	4/1	**93.5**	30.2	3/15	**2.52**	19.5	45.7	**53.4**	12/4	0.00
5th Largest	6/20	**79.0**	38.0	4/18	**0.91**	38.0	43.1*	**41.4**	6/26	0.00
10th Largest	5/16	**61.5**	20.4	5/22	**0.41**	30.2	38.1	**34.9**	2/9	0.00
20th Largest	5/13	**45.4**	27.9	12/4	**0.00**	53.4	33.0	**30.4**	6/27	0.00
50th Largest	3/29	**22.4**	11.1	7/28	**0.00**	26.0	25.4	**24.5**	2/15	0.00

* NOAA 25-year event and CLIGEN 20-year event

Table 3. Effects of the different spatial arrangements on runoff, hillside erosion, and sediment delivery for single sets of low and high severity soil properties. The table is in descending order by erosion rate.

Erosion Risk	Distribution	Runoff (mm)	Erosion (Mg ha^{-1})	Sed Yield (Mg ha^{-1})
High	HHH	22.7	77.0	73.0
High	LHH	20.9	66.2	61.5
High & Mod	HHL	17.2	56.8	30.7
High & Mod	HLH	17.5	54.5	52.1
Mod & Low	LHL	14.6	44.5	25.1
Mod & Low	LLH	14.9	38.4	36.7
Low	HLL	14.4	14.5	13.6
Low	LLL	11.9	4.6	4.4

precipitation. A 60-mm rainfall event is about a 100-year event based on CLIGEN and the NOAA maps (table 2). Table 3 is ordered by upland erosion rates, and apparently the order is

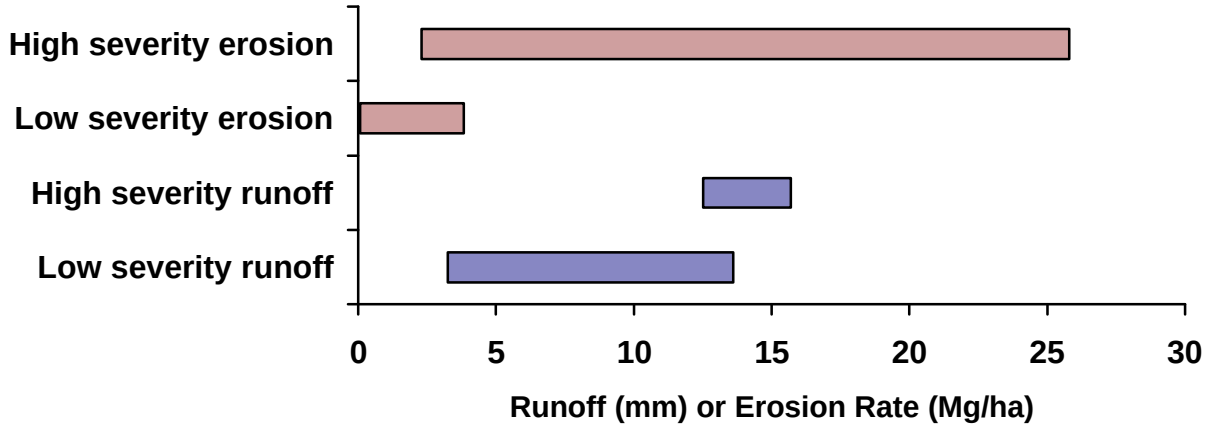

Figure 2. Effects of fire severity on predicted ranges of runoff and soil erosion for a 100-m long, 40 percent slope hill, with a 60-mm, 6-hr storm.

not the same for erosion as it is for sediment yield. A reasonable conclusion from this table is that the range of soil erosion rates due to spatial variability only is 55 to 77 Mg ha^{-1} for a high risk fire, 38 to 57 Mg ha^{-1} for a moderate risk fire, and 5 to 45 Mg ha^{-1} for a low risk fire from a 60-mm precipitation event.

Soil Variability Soil properties were varied over the range of values for low and high severity conditions presented in Table 1, for a 100-m long, 40 percent slope hill, with a 60-mm, 6-hr storm. Figure 2 shows the results of these runs, with low severity predicted erosion rates varying from 0.06 to 3.8 Mg ha^{-1}, and high severity rates from 2.3 to 25.8 Mg ha^{-1} for a 60-mm 6-h storm. Note that the range of predicted erosion rates is greater than two magnitudes. As a comparison, observed erosion rates from a 13-mm storm following the spring after a high severity fire were zero and 0.19 Mg ha^{-1} in a study in progress in the Wenatchee National Forest in Central Washington, and annual totals were zero and 4.4 Mg ha^{-1} on a 30 percent slope for two adjacent plots in the Wallowa-Whitman National Forest in Eastern Oregon the first year after a severe fire. Figure 2 also shows that there is an overlap in the distributions of both runoff and

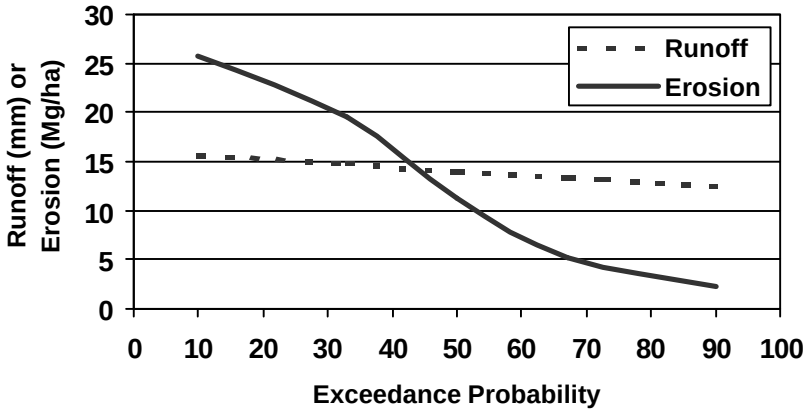

Figure 3. Example of output from the proposed fire risk interface.

erosion rates between high and low severity.

DISCUSSION

The results that are presented as a range in figure 2 can also be presented as exceedance values (figure 3). One of the challenges for the proposed application is that by selecting a design storm, the user has already limited predicted erosion to a very small set of storms. The results presented in figure 3 are associated with a 100-year precipitation event. Figure 3 shows that there is a ten percent chance in the year following a fire that erosion will exceed 26 Mg ha^{-1} storm, and a 90 percent chance that runoff will be less than 16 mm and erosion less than 26 Mg ha^{-1} from a 100 year storm event.

INTERFACES

To incorporate climate variability, spatial variability, and soil variability into erosion prediction is complex and time consuming with the current erosion models, including WEPP. Current models do not incorporate the ability to carry out return period analysis of storms. For each spatial arrangement and each soil condition a separate run or calculation is required. We are currently developing an interface that will allow the user to select or specify a storm, a soil textural category, a level of erosion risk, and slope length and steepness. The interface will then carry out several hundred computer runs for the given level of fire risk, and present the user with a table or graph such as that in figure 3, interpreting the results of the likelihood of soil erosion exceeding a given amount (Robichaud et al. 2000).

SUMMARY

Variability is a dominant factor in soil erosion prediction on forest landscapes. Variables include climate, soil properties, and the spatial distribution of fire severity. The range of erosion rates can vary by over a magnitude due to spatial variability, and over two magnitudes due to soil variability. A computer tool is under development to aid managers in evaluating the runoff and erosion risks associated with wildfire for a given storm.

REFERENCES

Elliot, W. J., Liebenow, A. M., Laflen, J. M., Kohl, K. D., 1989, A compendium of soil erodibility data from WEPP cropland soil field erodibility experiments 1987 & 88. NSERL Report No. 3. Columbus, OH: The Ohio State University, and W. Lafayette, IN: USDA Agricultural Research Service, 319 p.

Elliot, W. J., Hall, D. E., 1997, Water Erosion Prediction Project (WEPP) forest applications. General Technical Report INT-GTR-365. Ogden, UT: USDA Forest Service, Rocky Mountain Research Station, 11 p.

Flanagan, D. C., Livingston, S. J. (eds.), 1995, *WEPP User Summary*. NSERL Report No. 11, W. Lafayette, IN: National Soil Erosion Research Laboratory, 131 p.

Flanagan, D. C., Meyer, C. R., Yu, B., Scheele, D. L., 2001, Evaluation and enhancement of the CLIGEN weather generator. Proceedings of the ASAE International Symposium on Soil Erosion Research for the 21st Century. Honolulu, HI. Jan. 3-5, 2001. St. Joseph, MI: ASAE, 4 p.

Haan, C. T., 1994, *Statistical Methods in Hydrology.* Ames, IA: Iowa State University Press, 378 p.

Laflen, J. M., Elliot, W. J., Flanagan, D. C., Meyer, C. R., Nearing, M. A., 1997, WEPP–Predicting water erosion using a process-based model. *Journal of Soil and Water Conservation* 52(2), 96-102.

National Oceanic and Atmospheric Admin. (NOAA), 1973, NOAA Atlas 2, Volume V – Idaho. Precipitation-frequency Atlas of the Western United States, Available online at <http://www.wrcc.dri.edu/pcpnfreq.html>.

Nicks, A. D., Lane, L. J., Gander, G. A., 1995, Chapter 2. Weather Generator. In Flanagan, D. C., Nearing, M. A., *USDA-Water Erosion Prediction Project Hillslope Profile and Watershed Model Documentation.* W. Lafayette, IN: USDA Agricultural Research Service, 2.1-2.22.

Robichaud, P. R., 2000, Fire effects on infiltration rates after prescribed fire in Northern Rocky Mountain forests, USA. *Journal of Hydrology* 231-232, 220-229.

Robichaud, P. R., Luce, C. H., Brown, R. E., 1993, Variation among different surface conditions in timber harvest sites in the Southern Appalachians. International Workshop on Soil Erosion, Proceedings. Moscow, Russia. West Lafayette, IN: The Center for Technology Transfer and Pollution Prevention, Purdue University, 231-241.

Robichaud, P. R., Miller, S. M., 2000, Spatial interpolation and simulation of post-burn duff thickness after prescribed fire. Accepted for publication in the *International Journal of Wildland Fire.*

Robichaud, P. R., Monroe, T. M., 1997, Spatially-varied erosion modeling using WEPP for timber harvested and burned hillslopes. Presented at the 1997 ASAE International Meeting, Minneapolis, MN. August 10-14. Paper No. 975015. St. Joseph, MI: ASAE, 8 p.

Robichaud, P. R., Elliot, W. J., Pierson, F. B., Wohlgemuth, P. M., 2000, Risk assessment of fuel management practices on hillslope erosion processes. In Neuenschwander, L. F., Ryan, K. C., (technical eds.) Proceedings from the Joint Fire Science Conference and Workshop. June 15-17, 1999. Boise, ID. Moscow, ID: University of Idaho 58-65.

Scheele, D. L., Elliot, W. J., Hall, D. E., 2001, Enhancements to the CLIGEN weather generator for mountainous terrain. Proceedings of the ASAE International Symposium on Soil Erosion Research for the 21st Century. Honolulu, HI. Jan. 3-5, 2001. St. Joseph, MI: ASAE, 4 p.

SEDIMENT LABORATORY QUALITY-ASSURANCE PROJECT: STUDIES ON METHODS AND MATERIALS

By J. D. Gordon, Hydrologist, U.S. Geological Survey, Denver, Colorado; C.A. Newland, Physical Scientist, ATA Services, Inc., Denver, Colorado; and J.R. Gray, Hydrologist, U.S. Geological Survey, Reston, Virginia

Abstract: In August 1996 the U.S. Geological Survey initiated the Sediment Laboratory Quality-Assurance project. The Sediment Laboratory Quality Assurance project is part of the National Sediment Laboratory Quality-Assurance program. This paper addresses the findings of the sand/fine separation analysis completed for the single-blind reference sediment-sample project and differences in reported results between two different analytical procedures.

From the results it is evident that an incomplete separation of fine- and sand-size material commonly occurs resulting in the classification of some of the fine-size material as sand-size material. Electron microscopy analysis supported the hypothesis that the negative bias for fine-size material and the positive bias for sand-size material is largely due to aggregation of some of the fine-size material into sand-size particles and adherence of fine-size material to the sand-size grains. Electron microscopy analysis showed that preserved river water, which was low in dissolved solids, specific conductance, and neutral pH, showed less aggregation and adhesion than preserved river water that was higher in dissolved solids and specific conductance with a basic pH. Bacteria were also found growing in the matrix, which may enhance fine-size material aggregation through their adhesive properties.

Differences between sediment-analysis methods were also investigated as part of this study. Suspended-sediment concentration results obtained from one participating laboratory that used a total-suspended solids (TSS) method had greater variability and larger negative biases than results obtained when this laboratory used a suspended-sediment concentration method. When TSS methods were used to analyze the reference samples, the median suspended-sediment concentration percent difference was –18.04 percent. When the laboratory used a suspended-sediment concentration method, the median suspended-sediment concentration percent difference was –2.74 percent. The percent difference was calculated as follows:

$$\text{Percent difference} = \left(\frac{\text{reported mass - known mass}}{\text{known mass}} \right) \text{X } 100 .$$

INTRODUCTION

The collection and analysis of fluvial sediment samples has been an integral part of hydrologic studies in the United States for over 100 years (Glysson, 1989). To support this sediment monitoring and research, the U.S. Geological Survey (USGS) operates laboratories for the analysis of the physical characteristics of sediment.

Working with the USGS Sediment Action Committee and the USGS Water Quality Service Unit in Ocala, Florida, the Branch of Quality Systems (BQS) distributed test samples as part of a pilot standard reference study in 1992 and 1994 (George and Schroder, 1996). Results of the pilot studies indicated that a standard reference-sample project was feasible and practical. Following the 1992 and 1994 pilot studies, the BQS continued to pursue the development and testing of a standard reference-sample project for measurement of physical sediment properties. In 1996, these efforts led to an external quality-assurance project to ensure that the physical sediment data produced or used by the USGS are of a known quality and are sufficient to provide long-term comparability and consistency. The Sediment Laboratory Quality-Assurance (SLQA) project began in August 1996 and is part of the National Sediment Laboratory Quality-Assurance (NSLQA) program. The NSLQA program focuses on all quantitative analyses done on water-sediment mixtures to derive concentrations and sand/fine separations. The program is composed of seven components: (1) a single-blind reference sediment-sample project, (2) a double-blind reference sediment-sample project, (3) data analysis and reporting for each laboratory on a national basis, (4) follow-up evaluations, (5) onsite laboratory evaluations, (6) documentation of laboratory quality-assurance plans and quality-control procedures, and (7) training in laboratory operational procedures. The SLQA project contains the first four parts of the NSLQA program and is intended to provide quantitative information on sediment-data quality to sediment-laboratory customers (U.S. Geological Survey Office of Surface Water Technical Memorandum No. 98.05, 1998).

Between August 1996 and September 1999, the BQS completed eight single-blind sediment laboratory intercomparison studies. In each study, a set of nine single-blind reference samples were sent to each participating laboratory for analysis of suspended-sediment concentration, sediment mass, and the separation of fine- and sand-sized material. One of the findings of the interlaboratory comparison studies was that fine-size material—particles with a median diameter less than 62 micrometers (µm)—results were negatively biased, whereas sand-size material—particles with a median diameter 63 to 125 µm—results were positively biased.

It was determined that the positive bias observed for sand-size material mass and the negative bias observed for fine-size material mass may be due to a small amount of fine-size material adhering to the sand-size grains, which increases the perceived sand-size material mass and decreases the fine-size material mass (Gordon and others, 1999). To better understand why the biases occurred, additional studies were initiated by the BQS. A set of samples was prepared using SLQA reference materials (spark-plug dust and South Dakota sand) and deionized water as the matrix. A sand/fine separation was completed using standard USGS methods (Guy, 1969). The sediment was viewed using a scanning electron microscope. The images showed (1) aggregation of the fine-size material, (2) adherence of the fine-size material to the sand-size material, and (3) bacteria growing in the sediment-water mixture.

Also as part of the SLQA studies, the BQS reviewed various laboratory sediment methods to evaluate which methods provide the best results. The BQS compared data produced using a total-suspended solids (TSS) method and a suspended-sediment concentration (SSC) method. One of the participating laboratories in the study typically performed analyses for a wastewater-treatment facility. In the first three studies in which this laboratory participated (97-1 to 98-1), the analyses were performed using the 19th edition of the "Standard Methods for the Examination of Water and Wastewater,"—2540B Total Solids Dried at 103-105^{o}C and 2540D Total Suspended Solids Dried at 103-105^{o}C (American Public Health Association, 1995). These two methods allowed the sediment sample to be subsampled. From the SLQA study, it was determined that methods that allow for subsampling can cause results to be significantly negatively biased.

RESULTS OF SAND/FINE SEPARATION ANALYSES

The BQS, distributed nine standard SLQA reference sediment samples semiannually to each participating sediment laboratory. Each sample mailed to the laboratories was identified as a quality-assurance sample. Upon completion of the analyses by the participating laboratories, the analytical results, along with the methods of analysis, were returned to the BQS. Analytical results from all sediment quality-control samples were compiled and statistically summarized by BQS personnel on an intra- and interlaboratory basis and entered into a national data base. The closer the percent difference was to zero, the more accurate the individual determination was considered to be. The percent differences for the mass of fine- and sand-size material were calculated for each participating laboratory as follows:

$$\text{Percent difference} = \left(\frac{\text{reported mass - known mass}}{\text{known mass}} \right) \text{X } 100 .$$

The magnitude of the median percent difference values for fine- and sand-size material mass generally diminished over the course of the first eight interlaboratory comparison studies (96-1 to 99-2). In the first study (96-1) the median percent difference for fine-size material mass was –6.56 percent and 18.53 percent for sand-size material mass. In study 99-2, the median percent difference for fine-size material mass was –2.69 percent and 2.20 percent for sand-size material mass. Results from the first eight studies showed that fine-size material mass was negatively biased, whereas sand-size material mass was positively biased (fig.1).

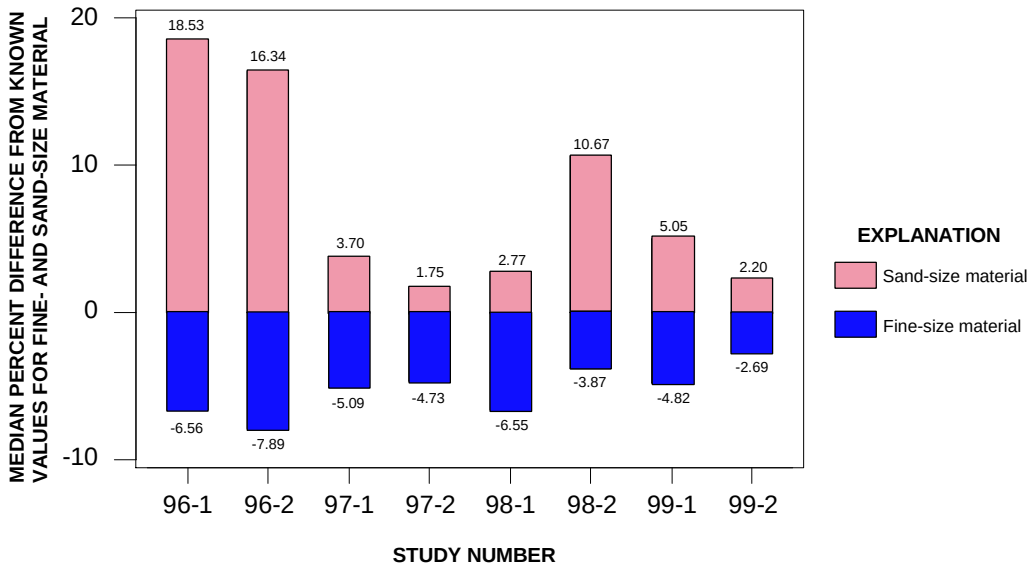

Figure 1. Results from studies 96-1 to 99-2 showing the biases for fine- and sand-size material.

SPECIAL STUDIES INVESTIGATING LABORATORY RESULTS

Aggregation of Particles: The spark-plug dust used in the SLQA project contained about 40 percent clay. Prior to hydration, these clay particles are negatively charged and are prevented from aggregating by the electrostatic repulsion between the electrical double layers. However, once hydrated, the layer of water on the surface prevents the particles from contacting each other. Coagulation can occur when electrostatic repulsion is reduced, such that clay particles of identical materials may now aggregate and form larger units (Manahan, 1994).

Two conditions within the water matrix must be fulfilled for aggregation of fine-size material to occur. Some process must bring particles close enough together to collide, and some of the collisions must result in coagulation. These mechanisms have been investigated in detail by many authors, such as Smoluchowski (1917), Friedlander (1965), Guy (1969), Krone (1978), Hunt (1980, 1982), Horowitz (1984, 1991), and Rao (1993). To build upon this earlier work, the BQS began studying sediment characteristics as they relate to the biases documented in the SLQA project.

Laboratory Bias Studies: In March 2000, the BQS, began the first SLQA special study. Nine sediment reference samples were prepared using SLQA reference materials with deionized water as the matrix. The samples were allowed to settle completely and then the supernatant liquid was removed to one inch above the sediment. Part of the reference material was then filtered using a 24-mm Whatman 934-AH filter[1], and part of the reference material was sieved using a 63-µm sieve to simulate a sand/fine separation.

The samples were dried at 105°C for 48 to 60 hours. The samples were taken to the Denver USGS microbeam laboratory, which operates a JEOL 5800 LV scanning electron microscope. The samples were mounted by laboratory personnel and placed under the scanning electron microscope. An example of fine- and sand-size material as they appeared under the electron microscope is shown in figure 2. Some of the fine-size particles aggregated to form particles about the same size as a sand-size particle, and some of the fine-size material adhered to the sand-size material, thereby diminishing the apparent amount of fine-size material and increasing the apparent amount of sand-size material. This may be one reason contributing to the biases documented in the SLQA project.

[1] Reference to trade names, commercial products, manufacturers, or distributors in this paper is for identification purposes only and does not constitute an endorsement or a recommendation for use by the U.S. Geological Survey.

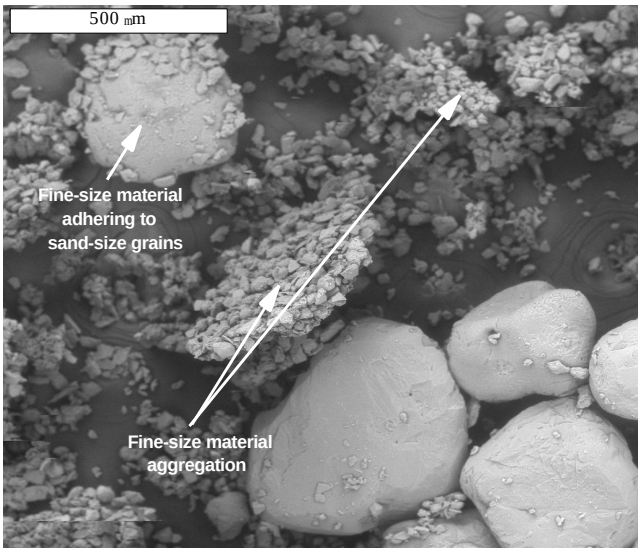

Figure 2. Scanning electron microscope image depicting the aggregation of fine-size material and adherence of fine-size material to sand-size grains.

A second study was conducted by the BQS in May 2000. In this study preserved river water replaced deionized water as the sample matrix. It was assumed that natural waters are never pure compared to the deionized water used in the SLQA project. The composition of the aqueous solution that is analyzed in sediment laboratories is a function of a multiplicity of factors, such as the initial composition of the water, the partial pressure of the gas phase, the type of mineral matter the water contacts, and the pH and oxidation potential of the solution (Fetter, 1988). If the water contains a biotic assemblage of any kind, then the chemistry of the water is even more complex. In this study (May 2000), spherical prokaryotes, Cocci bacteria (fig. 3) were detected in the river-water samples analyzed by the BQS. Most of the spherical prokaryotes found in these samples have cell walls that contain a unique material called peptidoglycan, which consists of polymers of modified sugars cross-linked by short polypeptides (Campbell, 1996). Peptidoglycan has adhesive properties, which may cause the clay particles to adhere to each other and to the sand-size material, thus potentially increasing the amount of sand-size material measured in laboratory analyses. After testing the fine- and sand-size materials, it was concluded that the bacteria were introduced into the river water when the fine-size material was added to the different river-water matrices. This may be a second reason why the biases documented in the SLQA project are occurring.

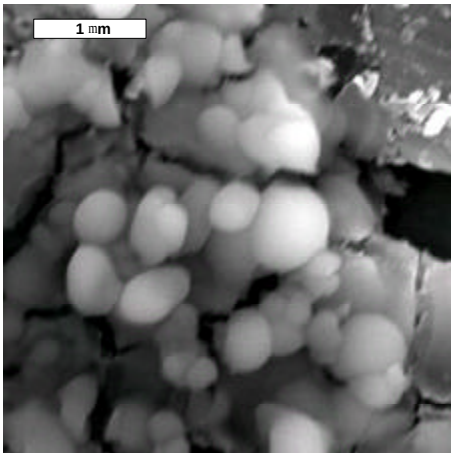

Figure 3. Scanning electron microscope depiction of Cocci bacteria (spherical prokaryotes) detected during analysis.

From the preserved river water used in the second study, dissolved-solids concentration, pH, and specific conductance were determined for each type of preserved river water. Each type of preserved river water used in the

second study (May 2000) had been sterilized by pumping it through 0.45-, 0.2-, and 0.1-µm filters, in series, into a 1,200-liter polypropylene drum. The water was continuously circulated and passed through a 0.1-µm filter and ultraviolet sterilizer for 24 hours. Following this circulation, the water was chlorinated to 5 parts per million free chlorine with sodium hypochlorite (NaOCl) (Farrar, 2000). After all the NaOCl had dissociated, a known amount of fine- and sand-size materials was added to each preserved river-water sample.

Three types of river water were used in the second study (May 2000). Type 1 river water contained 66.5 milligrams per liter (mg/L) dissolved solids, had a pH of 6.60, and a specific conductance of 113 microsiemens per centimeter (µS/cm). The samples were allowed to settle in solution for one week. The supernatant liquid was removed to about one inch above the sediment at the bottom of the jar. The sediment was wet-sieved using a 63-µm sieve to separate the fine- and sand-size mixture. The samples were dried at 105°C for 48 to 60 hours and examined at the scanning electron microscope laboratory. The images showed no aggregation of fine-size material and no adhesion of fine-size material to sand-size material (fig. 4).

In the second part of this study (May 2000), sand/fine reference material was added to two other types of river water: (1) type 2 river water contained 277 mg/L dissolved solids, had a pH of 8.09, and a specific conductance of 493 µS/cm, and (2) type 3 river water contained 689 mg/L dissolved solids, had a pH of 8.29, and a specific conductance of 1,076 µS/cm. The samples were allowed to settle for one week. After one week, the samples were wet-sieved using a 63-µm sieve to separate the fine-size material from the sand-size material. Images of these samples under the scanning electron microscope did show some aggregation (fig. 4).

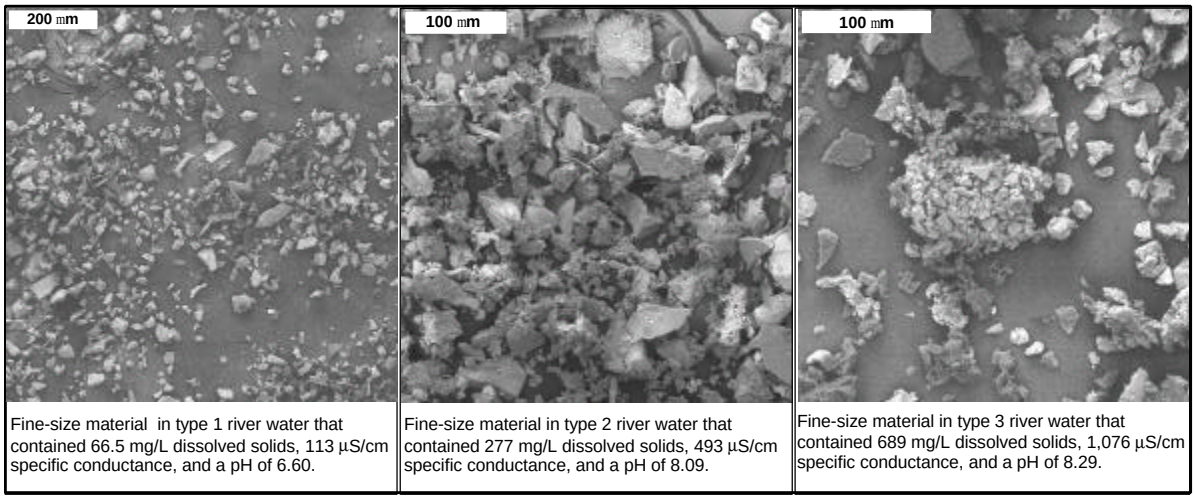

Figure 4. Scanning electron microscope images of three types of river water that were used in the second special study (May 2000). The far left picture shows sediment characteristics in river water 1, the middle picture shows sediment characteristics in river water 2, and the far right picture shows sediment characteristics in river water 3.

From the second special study (May 2000) it was concluded that variables that influence the amount of aggregation detected in these river-water samples may include water characteristics, such as the kind and concentration of dissolved constituents. An explanation for this finding may be that clay particles in the fine-size material may have attained a new negative charge by ion replacement, in which Si(IV) and Al(III) ions were replaced by metal ions of similar size, but lesser charge. Compensation would have been made for this negative charge by association of cations with the clay surfaces. Since these cations need not fit specific sites in the crystalline lattice of the clay, they may be relatively large ions, such as potassium (K^+) or sodium (Na^+) (Manahan, 1994). For grain-to-grain interactions, it is very possible that multivalent metal ions, such as magnesium (Mg^{2+}) and calcium (Ca^{2+}), could act as convenient agents to cement grains together (Rao, 1993).

COMPARISON OF TWO METHODS FOR DETERMINING SUSPENDED-SEDIMENT CONCENTRATIONS

The best methods for making determinations of concentrations from suspended-sediment samples must be selected from numerous possible procedures. One participating laboratory analyzed quality-control samples (97-1 to 98-1) using Method 2540D, known as a total-suspended solids (TSS) method, of the American Public Health Association, American Water Works Association, and Water Pollution Control Federation (1995) with the following variation: instead of removing the subsample with a pipette, the sample was shaken vigorously and one-third of the desired subsample volume was decanted to a secondary vessel. This process was repeated twice to obtain a single subsample for subsequent filtering, drying, and weighing. Beginning with the second study in 1998 (98-2), the participating laboratory used the American Society for Testing and Materials (ASTM) designation D3977-80, "Standard Practice for Determining Suspended-Sediment Concentration in Water Samples" (American Standards for Testing and Materials, 1980), which was adapted generally from a report of the U.S. Inter-Agency Committee on Water Resources, Subcommittee on Sedimentation and H.P. Guy (Guy, 1969); this is referred to as a suspended-solid concentration (SSC) method and is equivalent to the method used by the USGS (fig. 5).

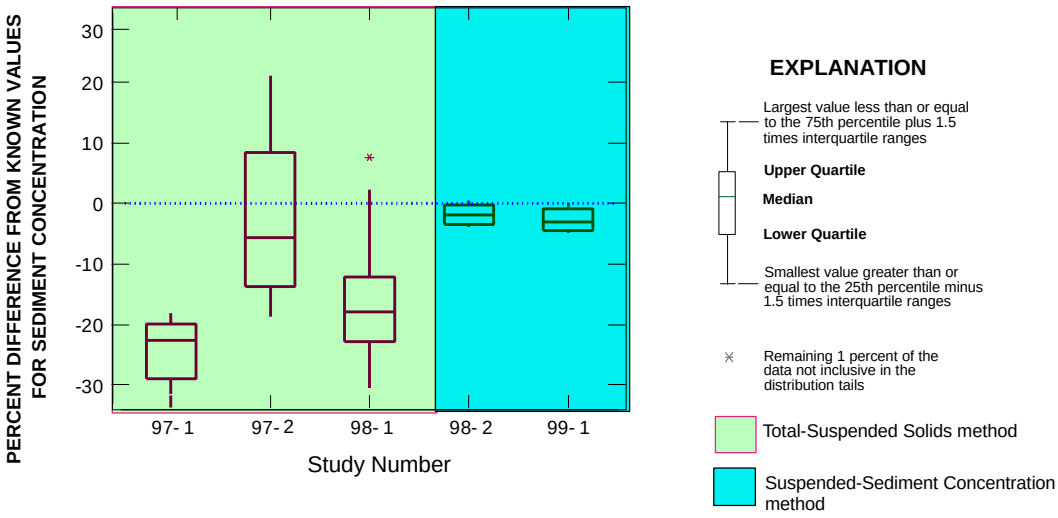

Figure 5. Results of percent differences from known values for sediment concentrations obtained using a total-suspended solids method and a suspended-sediment concentration method used by a participating laboratory. Studies 97-1 through 98-1 were conducted using a total-suspended solids method. Studies 98-2 and 99-1 were conducted using a suspended-sediment concentration method.

When reviewing the results, shown in figure 5, it was determined that the methods for analyzing TSS, which allow subsampling, may not be applicable to suspended-sediment analyses. Suspended inorganic particles in river water generally have a high specific gravity of about 2.65, which makes it difficult to obtain a representative subsample. Large sediment particles settle too swiftly to be subsampled accurately by pouring or pipetting. For example, the fall rate for a 0.125-millimeter sand-size particle is about 1 centimeter per second (Guy, 1969). The pint-size bottles sent to the participating laboratory contained 200 milliliters of water or about 6 vertical centimeters of water. If, after shaking or stirring the sample, a sand-size particle began at the top of the water, it would take only 6 seconds for the particle to fall to the bottom of the bottle. This high fall rate makes accurate subsampling almost impossible.

An evaluation of data collected and analyzed by the USGS and others has shown that the variation in TSS analytical results is considerably larger than that for traditional SSC analytical results and that the TSS data for the participating laboratory had a larger amount of variability and in general a negative bias when compared to SSC data (Gray and others, 2000, Glysson and others, 2000). The inability to produce a representative amount of sand-size material in a subsample is one reason why the TSS values differ substantially from SSC values (Glysson and others, 2000).

CONCLUSIONS

A negative bias for fine-size material mass and a positive bias for sand-size material mass were consistently found in the Sediment Laboratory Quality-Assurance (SLQA) project's first eight studies (96-1 to 99-2). Because of these findings, the U.S. Geological Survey (USGS) Branch of Quality Systems began conducting a series of special studies starting in March 2000. The initial results of these special studies indicated that the biases observed during the SLQA project may be due to the fine-size material aggregating to form larger particles that did not pass through the 63-micrometer sieve and fine-size material adhering to the sand-size material grains. When reviewing photographs of the sediment material grains, which were taken using a scanning electron microscope, the sediment samples from the initial study (March 2000) appeared to show that the aggregation was intensified when deionized water was used as the matrix.

To further study how sediment reacts with different types of water, preserved river water was used as the sample matrix in the second study (May 2000). Initially it was found that when the sample matrix had a neutral pH, a low specific conductance, and a small dissolved-solids concentration, there appeared to be no aggregation of the fine-size material and no adherence of the fine-size material to the sand-size material. However, when the sample matrix contained higher dissolved solids, higher specific conductance, and had a basic pH, the fine-size material showed some aggregation when viewed under the scanning electron microscope. Conclusions drawn from these results would indicate that the pH and dissolved constituents in the water affect the amount of coagulation of the sediment in solution.

Bacteria were observed growing in the preserved river-water matrix during the second study (May 2000). These bacteria were assumed to exert an important influence in the coagulation of the fine-size material because their cells consist of polymers of modified sugars cross-linked by short polypeptides. It was concluded from observing these bacteria that a fuller understanding of the characteristics of fine-grained sediment-bacterial complexes is needed.

If the bias observed in the SLQA studies is caused either by bacteria, preserved river water matrix effects, or both, then similar biases could be affecting the sand/fine separations performed in the USGS sediment laboratories. From the results of these initial studies, it is apparent that these and other sediment-water characteristics need further study and that an integrated multidisciplinary approach is needed to understand the complex characteristics of sediment and bacteria.

Differences between sediment analysis methods were investigated as part of the SLQA project. A laboratory participating in the project produced sediment concentration data by using a total-suspended solids (TSS) method, which allows subsampling. Because the results of the participating laboratory were consistently biased negatively and varied significantly when compared to other participating laboratories that used a suspended-sediment concentration (SSC) method, the laboratory changed its method to the SSC method, which is equivalent to the method used by the USGS. A conclusion from this study was that the differences between TSS and SSC analyses can be significant and that further study of the differences between these two methods is warranted.

REFERENCES

American Public Health Association, 1995, Standard Methods for the Examination of Water and Wastewater—2540B, Washington, D.C., p. 2-53-2-56.

American Standards for Testing and Materials (ASTM) [Designation 2540D], 1980, D-3977-80, Standard [Practice] Test Method for Determining Suspended-Sediment Concentration in Water Samples, Philadelphia, ASTM, v. 31, p. 1264-1272.

Campbell, Neil A., 1996, Biology: The Benjamin/Cummings Publishing Company, Inc., p. 500-501.

Farrar, Jerry W., 2000, Results of the U.S. Geological Survey's analytical evaluation program for standard reference samples distributed in October 1999, U.S. Open-file report 00-227, p. 6.

Fetter, C.W., 1988, Applied hydrogeology: New York, Macmillan Publishing Company, p. 576.

Friedlander, S.M., 1965, The similarity theory of the particle size distribution of the atmospheric aerosol: Czechoslovakia Academy of Science, Prague, p. 115-130.

George, John R., and Schroder, LeRoy J., 1996, Sediment Laboratory Quality: Are You Assured? Proceeding of the Sixth Federal Interagency Sedimentation Conference, March 10-14, 1996, Las Vegas, Nevada, p. 18-25.

Glysson, G. D., 1989, 100 Years of sedimentation study by the USGS, in Sediment Transport Modeling: Proceeding of the International Symposium, American Society of Civil Engineers, August 14-18, 1989, New Orleans, Louisiana, p. 827-829.

Glysson, G. D., Gray, John R., and Conge, Lisa M., 2000, Adjustment of total suspended solids data for use in sediment studies, Proceedings of ASCE's 2000 Joint Conference on Water Resources Engineering and Water Resources Planning and Management, July 30 - August 2, 2000, Minneapolis, MN, 10 p.

Gordon, John D., Newland Carla A., and Gagliardi, Shane T., 1999, Laboratory performance in the Sediment Laboratory Quality-Assurance Project, 1996-1998: U.S. Geological Survey Water-Resources Investigations Report 99-4189, p. 8-31.

Gray, J.R., Glysson, G.D., Turcios, L.M., and Schwarz, G.E., 2000, Comparability of total-suspended solids and suspended-sediment concentration data: U.S. Geological Survey Water-Resources Investigations Report 00-4191, 14 p.

Guy, Harold P., 1969, Laboratory theory and methods for sediment analysis: U.S. Geological Survey Techniques of Water Resources Investigations, book 5, chap. C1, 58 p.

Horowitz, Arthur J., 1984, A primer on trace metal-sediment chemistry: United States Geological Survey, Open-file report 84-709, p. 14-41.

Horowitz, Arthur J., 1991, A primer on sediment-trace element chemistry, 2nd edition: United States Geological Survey, Open-file report 91-76, p. 30-31.

Hunt, J.R., 1980, Prediction of oceanic particle size distributions from coagulation and sedimentation mechanisms, Particulates in Water, American Chemical Society, Advances in chemistry series, No 189, p. 243-257.

Hunt, J.R., 1982, Self similar particle-size distributions during coagulation: theory and experimental verification, Fluid Mechanisms, No. 122, p. 169-186.

Krone, R.V., 1978, Aggregation of suspended particles in estuaries, Estuarine Transport Processes, University of South Carolina Press, Columbia, South Carolina, p. 177-190.

Manahan, Stanley E., 1994, Environmental chemistry: Ann Arbor, Lewis Publishers, p. 441-443.

Rao, Salem S., 1993, Particulate matter and aquatic contaminants, Ann Arbor, Lewis Publishers, p. 199.

Smoluchowski, M., 1917, Versuch einer mathematishen Theorie der Koagulation kinetik killoider Losugen, Ann. Physik Chemistry, p. 129-168.

U.S. Geological Survey, 1998, A national quality assurance project for sediment laboratories operated or used by the Water Resource Division: U.S. Geological Survey, Office of Surface Water Technical Memorandum No. 98.05, issued March 2, 1998, at URL http://water.usgs.gov/admin/memo/SW/sw98.05.txt

---

Much appreciation is extended to Doug Glysson and Pete Rogerson for their contributions to this report.

GCLAS: A GRAPHICAL CONSTITUENT LOADING ANALYSIS SYSTEM

By T. E. McKallip, Hydrologist, U.S. Geological Survey, Reston, Virginia; G. F. Koltun, Hydrologist, U.S. Geological Survey, Columbus, Ohio; J. R. Gray, Hydrologist, U.S. Geological Survey, Reston, Virginia; G. D. Glysson, Hydrologist, U.S. Geological Survey, Reston, Virginia

Abstract: The U. S. Geological Survey has developed a program called GCLAS (Graphical Constituent Loading Analysis System) to aid in the computation of daily constituent loads transported in stream flow. Due to the relative paucity with which most water-quality data are collected, computation of daily constituent loads is moderately to highly dependent on human interpretation of the relation between stream hydraulics and constituent transport. GCLAS provides a visual environment for evaluating the relation between hydraulic and other covariate time series and the constituent chemograph. GCLAS replaces the computer program Sedcalc, which is the most recent USGS sanctioned tool for constructing sediment chemographs and computing suspended-sediment loads. Written in a portable language, GCLAS has an interactive graphical interface that permits easy entry of estimated values and provides new tools to aid in making those estimates. The use of a portable language for program development imparts a degree of computer platform independence that was difficult to obtain in the past, making implementation more straightforward within the USGS' s diverse computing environment. Some of the improvements introduced in GCLAS include (1) the ability to directly handle periods of zero or reverse flow, (2) the ability to analyze and apply coefficient adjustments to concentrations as a function of time, streamflow, or both, (3) the ability to compute discharges of constituents other than suspended sediment, (4) the ability to easily view data related to the chemograph at different levels of detail, and (5) the ability to readily display covariate time series data to provide enhanced visual cues for drawing the constituent chemograph.

INTRODUCTION

The Graphical Constituent Loading Analysis System (GCLAS) is a program developed by the U. S. Geological Survey (USGS) to facilitate the interactive visualization and editing of water-quality constituent time-series data and the computation of daily constituent loads. GCLAS replaces Sedcalc (Koltun and others, 1994), an earlier USGS program designed to assist in the computation of suspended-sediment loads. Written in the portable language JAVA[1], GCLAS does not represent a new methodology for the computation of constituent loads, however, it does provide an integrated set of tools designed to support analyses and computational methods that previously were done manually (or by some other means, depending in large part on the capabilities and resources available to the analyst). JAVA was specifically designed to facilitate cross-computer-platform compatibility of code and thus was a logical choice for use in the USGS' s diverse computing environment.

GCLAS automates many formerly manual aspects of determining constituent loads, in part by dynamically linking an assortment of graphical and tabular views of water-quality and discharge data. The linking of different data views creates an environment that will aid interpretation of the interaction between stream hydraulics and constituent transport. This environment also eliminates or simplifies many procedural tasks associated with plotting and calculations and, consequently, should result in more efficient and cost-effective and accurate analyses.

PROGRAM FEATURES

Data Input: Several data input formats are supported by GCLAS. Specifically, GCLAS can read streamflow and water-quality time-series data in the USGS National Water Information System, NWIS (USGS, http://wwwnwis.er.usgs.gov) unit-values card-image format, in named column tab-delimited ASCII format, in the Sedcalc "sedata" format, and in a format output by the USGS' sediment-laboratory software, SLEDS (USGS, http://vulcan.wr.usgs.gov/Projects/SedLab/SLEDS/).

Display Features: Once data have been imported into GCLAS, the user is presented with a multi-panel display showing the data in both graphical and tabular formats (fig. 1). All panels and windows in GCLAS can be resized, and zoom controls are provided in graph panels to adjust the magnification of the view and the resolution of the cursor coordinates.

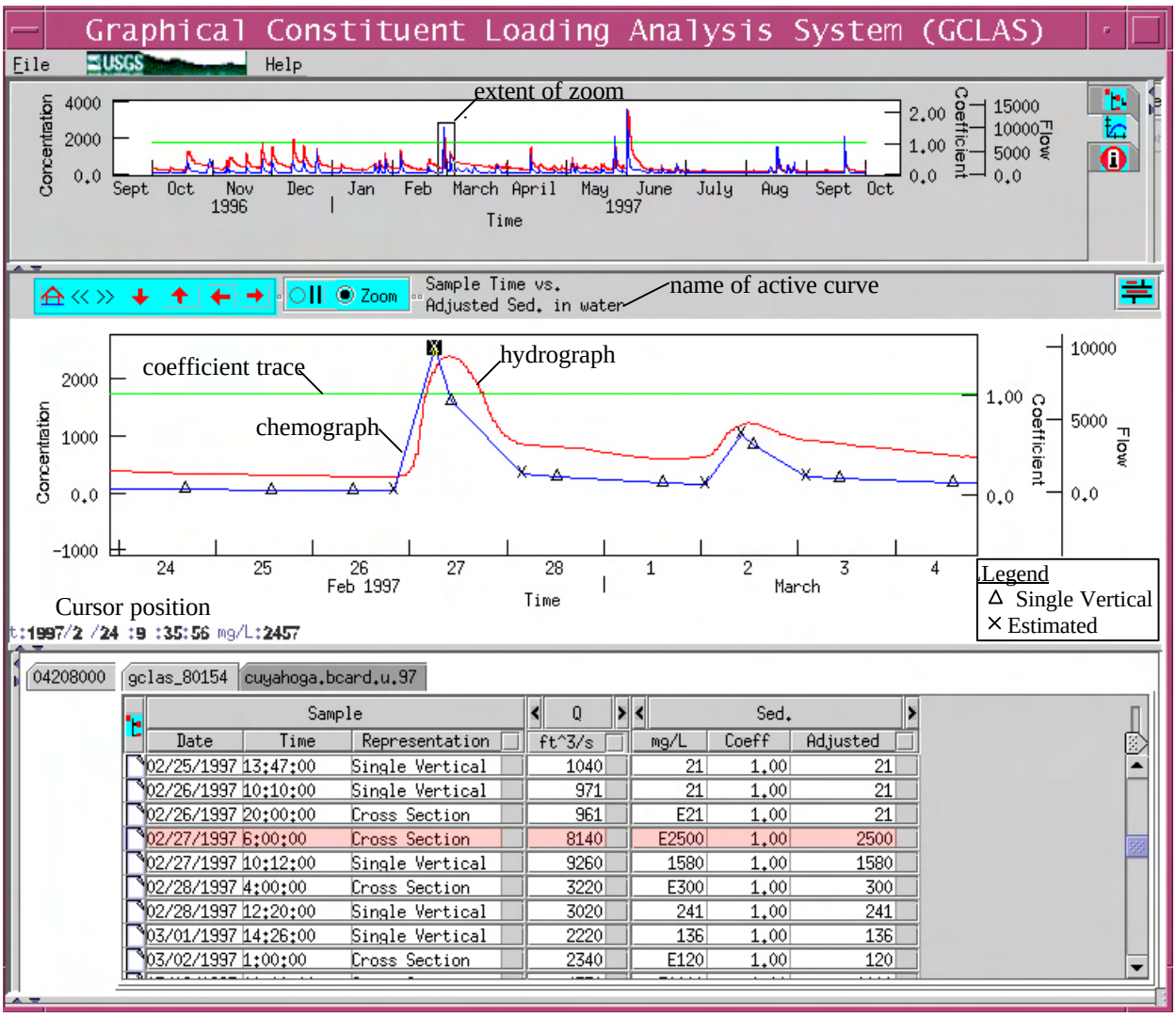

Figure 1 Annotated screen shot of a multi-panel display in GCLAS

The static nature of the predecessor program, Sedcalc, forced the use of logarithmic scales on graphs that led to programmatic restrictions on zero and negative flows, and on zero- valued concentrations. The ability to readily and dynamically rescale graphs in GCLAS facilitated use of arithmetic coordinates, thus eliminating the need for artificial restrictions on flow and concentration values.

Data measured at locations other than the site of interest or at the same site but for a different water year can be imported into GCLAS and simultaneously be displayed to facilitate hydrographic comparisons. Data from different water years are automatically offset in time so that they can be displayed on the scale of the active water year. Discrete water-quality data values are shown on the graphs using different symbols, depending on whether they are considered to represent (a) measurements that are not representative of average conditions for the stream cross section, (b) measurements that are representative of average conditions for the stream cross section, or (c) estimated concentrations or conditions.

Tabular data are presented in panels using a tabbed-folder format in which different types of data and data from different sites (or the same site for different years) are organized under separate tabbed tables (fig. 2). Switching between tables is accomplished by selecting the appropriate tab. Depending on the type of data contained in a table, a considerable amount of ancillary information may be associated with each data value. For instance, concentration data may have associated ancillary information on the method of measurement, the coincident hydrologic conditions, quality-assurance information, and so forth. Whereas ancillary information of that sort may be important for some analyses, that information may serve merely as a distraction for other analyses. Consequently, GCLAS was designed to permit ancillary information to be temporarily hidden from view. The user can toggle between detailed and less-detailed views of data by double-clicking on major or minor table headings in the tabbed views. GCLAS provides additional data-viewing flexibility by permitting columns to be reordered by simply dragging a column heading to its desired location within the table.

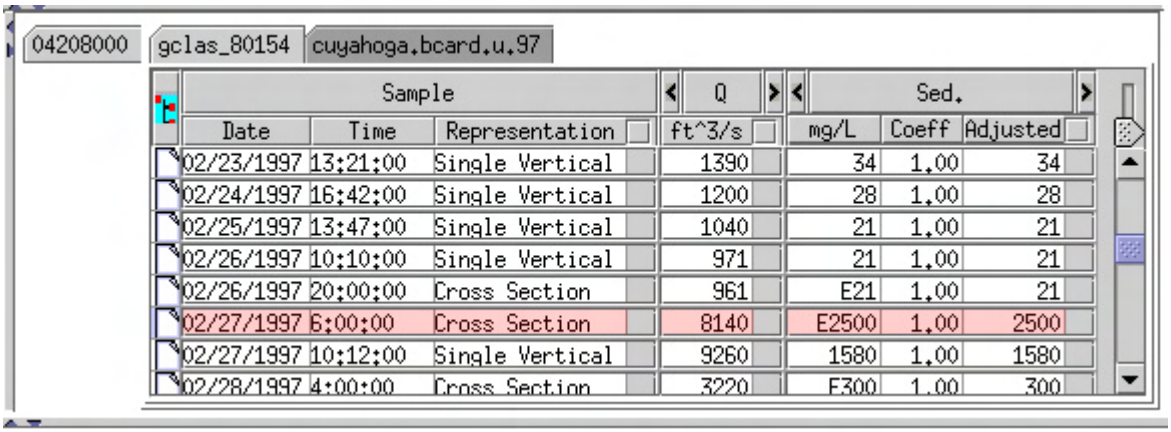

Sample			Q	Sed.		
Date	Time	Representation	ft^3/s	mg/L	Coeff	Adjusted
02/23/1997	13:21:00	Single Vertical	1390	34	1.00	34
02/24/1997	16:42:00	Single Vertical	1200	28	1.00	28
02/25/1997	13:47:00	Single Vertical	1040	21	1.00	21
02/26/1997	10:10:00	Single Vertical	971	21	1.00	21
02/26/1997	20:00:00	Cross Section	961	E21	1.00	21
02/27/1997	6:00:00	Cross Section	8140	E2500	1.00	2500
02/27/1997	10:12:00	Single Vertical	9260	1580	1.00	1580
02/28/1997	4:00:00	Cross Section	3220	E300	1.00	300

Figure 2. Example of tabular data view in GCLAS' s tabbed-folder format.

Data shown in graphs and tables are dynamically linked so that modifications to data in one view are automatically reflected in the other views. For example, if an estimated concentration value is modified in the table view, its position in the graph view is automatically updated. Also, double-clicking on a

discrete value symbol in the graph view triggers synchronization of the table view with the corresponding discrete-value entry highlighted.

Cross-section Coefficients: For a given constituent, the mean concentration in the stream cross section must be known in order to compute accurate loads as a function of the total flow in the stream. Depending on the combination of technique and sampler used to collect the water-quality sample, the concentration of the constituent in the sample may or may not be representative of the mean concentration in the cross section. When measured concentrations are not representative of the mean concentration, it becomes necessary to apply a coefficient to the measured concentration value in order to obtain a value that is more representative of the mean. These coefficients are commonly referred to as cross-section coefficients (fig. 1).

When water-quality samples are collected routinely at a site for the purpose of computing daily loads, it is common to collect the majority of samples in a fashion that can (at times) yield concentrations that differ from the cross-sectional mean (for example, when operating a fixed-intake pumping sampler). In those situations, the USGS collects periodic depth- and width-integrated isokinetic samples coincident with samples obtained by means of the routine method (for example the pumping sampler). The depth- and width-integrated samples should yield concentrations that are representative of the mean concentration in the cross section and, consequently, can be compared to the routine sample to assess trends in the relation between concentrations from the routine samples and the corresponding mean concentrations. The ratio of the concentration measured in a given depth- and width-integrated sample to the concentration measured in the corresponding routine sample is the cross-section coefficient for that sample set. Therefore if the cross-section coefficient is multiplied by the routine sample concentration, then the concentration of the depth- and width-integrated sample is obtained (the best measure of the mean concentration in the cross section).

GCLAS provides a variety of tools to aid in (a) computing the cross-section coefficients, (b) assessing trends in the coefficients, and (c) visualizing and applying coefficient relations. Once coefficients have been determined in GCLAS, graphs of coefficients as a function of time and coefficients as a function of streamflow can be easily displayed; this permits a quick visual assessment of these common trend relations (fig. 3). Ultimately, GCLAS provides tools to define and apply coefficient relations as a constant function or as a function of time, streamflow, or a combination of the two.

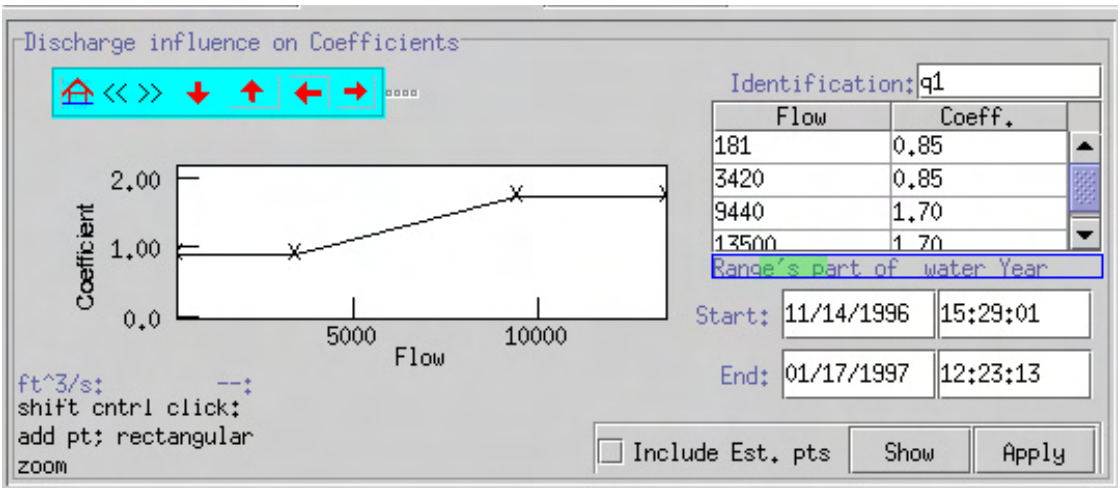

Figure 3. Screen shot of a GCLAS view used to visualize coefficient relations to streamflow.

Construction of cross-section coefficient relations can be complex, particularly when coefficients vary as a function of both time and streamflow. To help the analyst visualize the result of application of the coefficient relation, GCLAS computes a coefficient time series and displays it as a separate curve in the graph-view window. GCLAS also reports computed coefficients in the tabular view and provides special tools that permit the analyst to easily determine the coefficient that would be applied for hypothetical streamflows and (or) points in time.

Transport Curves: To compute accurate loads, the analyst must ensure that the constituent time series is drawn accurately. Because of limited resources, constituent time series are rarely measured at ideal temporal frequencies. Most commonly, the constituent time series is sampled relatively infrequently, requiring the analyst to "fill in" or estimate data for periods when measured data are lacking. Developing those estimates requires knowledge of the stream hydrology and of the transport characteristics of the constituent of interest.

A transport curve, which is a plot of a water-quality constituent's concentrations (or loads) as a function of the coincident streamflows, is a tool commonly used to assess a constituent's transport characteristics. GCLAS has an integral transport-curve window that shows streamflow as a function of concentration characteristics for the measured data in the data set. Transport curves commonly show some variability in measured concentration for a given streamflow. That variability may be due to variation in antecedent basin moisture conditions, variation in the distribution of rainfall amounts or intensities within the basin, or a variety of other factors. Because of that variability, the analyst must consider other factors or cues when developing concentration estimates. GCLAS displays cross hairs in the transport-curve window(fig. 4a) that intersect at coordinates that are a function of the position of the cursor in the time-series graph view (fig. 4b). Specifically, the streamflow (X) coordinate (fig.4a) is set to the streamflow that is coincident in time with the position of the cursor in the time-series graph view (fig. 4b) and the concentration (Y) coordinate is set to the concentration value corresponding to the position of the cursor in the time-series graph view. The cross-hair display facilitates estimating missing values by allowing the analyst to consider ancillary factors and cues (such as the measured recession characteristics), and at the same time see how closely alternative estimates fit with previously observed transport characteristics.

Estimated Values: Estimated values can be added in the working graph view by holding down the shift and control keys and pressing the left mouse (or pointer) button. The X and Y coordinates of the cursor in the working graph view are continuously tracked and displayed in the lower left corner of the panel. The coordinate information is particularly useful when graphically adding estimated values to help ensure that estimates are added at the desired coordinates. If an estimate is added and later judged to be incorrect, it can be removed, disregarded, or its concentration coordinate can be modified either by dragging the point vertically (up or down) in the working graph window or by editing the concentration in the tabular view. Values that are marked as disregarded are shown on the graphs and tables but are disregarded for all other display and computational purposes.

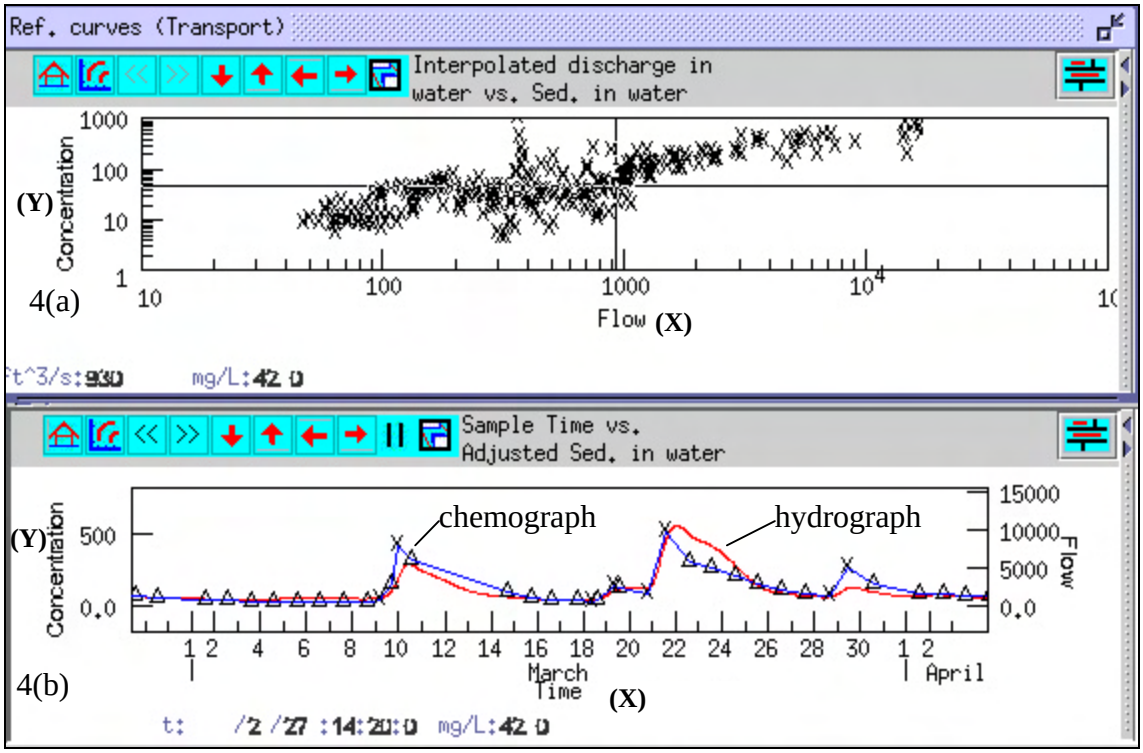

Figure 4. Annotated screen shot showing (a) the linked transport curve and (b) graph view panels from GCLAS.

Load Computation: At any time during the record working process, daily, monthly and annual loads can be calculated in GCLAS, literally at the press of a button. Calculations are performed by application of the mid-interval method (Porterfield, 1972) to concentration data that are interpolated to the same temporal frequency as the unit-streamflow data. If desired, calculations can be easily repeated to test the affect of alternative analysis strategies on computed loads.

GCLAS has the potential to compute loads for any constituent that is transported in water at measurable concentrations. At present, GCLAS contains no provision to handle censored ("less-than")

data explicitly in the load calculation algorithm and, consequently, should not be used to compute loads of constituents that have an appreciable amount of censored values.

PROGRAM AVAILABILITY AND PLANS

GCLAS was released to internal USGS customers in beta form in October, 2000. The program is distributed by means of the USGS Hydrologic Analysis Software Support (HASS) Program web page at http://water.usgs.gov/hass/. Public release of GCLAS is planned for early 2001 with the HASS web page acting as the main distribution point. Additional features are planned for the public release, including the ability to estimate concentrations by application of a user-defined equation, improved report capabilities, and addition of an integrated data base.

[1] The use of brand, trade, or firm names in this paper is for identification purposes only and does not constitute endorsement by the U.S. Government.

REFERENCES

Koltun, G. F., Gray, J. R., and McElhone, T. J., 1994, User's manual for SEDCALC, A computer program for computation of suspended-sediment discharge, U. S. Geological Survey Open-File Report 94-459, 46 p.

Porterfield, George, 1972, Computation of fluvial-sediment discharge: U. S. Geological Survey Techniques of Water Resources Investigations Book 3, Chapter C3, 66 p.

USGS, National Water Information System (NWIS) at URL http://wwwnwis.er.usgs.gov/

USGS, Sediment Laboratory Environmental Data System (SLEDS) at URL http://vulcan.wr.usgs.gov/Projects/SedLab/SLEDS/